Department of Neuroscience and Biomedical Engineering

Model-based exploration of interactions in the visual cortex

Fariba Sharifian

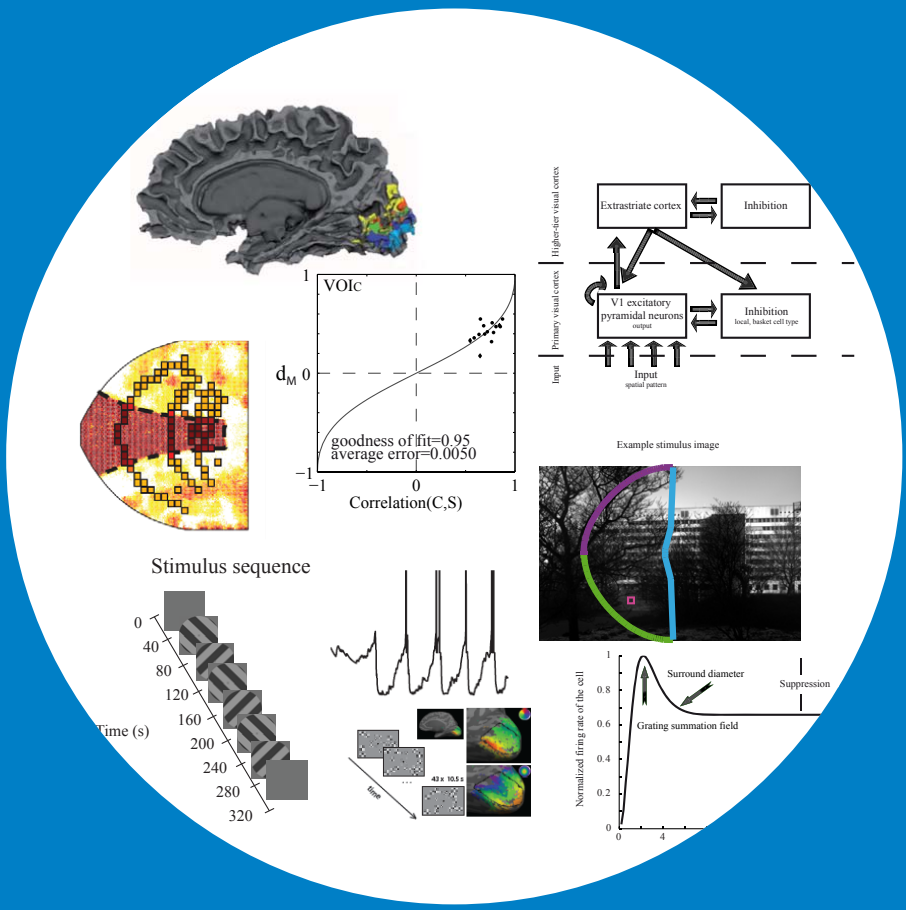

Aalto University

DOCTORAL DISSERTATIONS

Aalto University publication series
DOCTORAL DISSERTATIONS 193/2015

Model-based exploration of interactions in the visual cortex

Fariba Sharifian

A doctoral dissertation completed for the degree of Doctor of Science (Technology) to be defended, with the permission of the Aalto University School of Science, at a public examination held at the lecture hall F239a, Otakaari 3 on 16 December 2015 at noon.

Aalto University

Dept. Neuroscience and Biomedical Engineering, Aalto University
Dept. Clinical Neurosciences, University of Helsinki

Supervising professor
Professor Matti Hämäläinen, Department of Neuroscience and Biomedical Engineering, Aalto University, Finland

Thesis advisor
Doctor Simo Vanni, Clinical Neurosciences, Neurology, University of Helsinki and Helsinki University Hospital, Finland

Preliminary examiners
Professor Juha Voipio, Department of Biological and Environmental Sciences, University of Helsinki, Finland and
Doctor Teemu Rinne, Institute of Behavioural Sciences,University of Helsinki, Finland

Opponent
Professor Simon Thorpe, Centre de Recherche Cerveau et Cognition, CNRS and Université Paul Sabatier, France

Aalto University publication series
DOCTORAL DISSERTATIONS 193/2015

ISBN 978-952-60-6529-8 (printed)
ISBN 978-952-60-6530-4 (pdf)
ISSN-L 1799-4934
ISSN 1799-4934 (printed)
ISSN 1799-4942 (pdf)
http://urn.fi/URN:ISBN:978-952-60-6530-4

Unigrafia Oy
Helsinki 2015

Finland

441 697
Printed matter

Author
Fariba Sharifian

Name of the doctoral dissertation
Model-based exploration of interactions in the visual cortex

Publisher School of Science

Unit Department of neuroscience and biomedical engineering

Series Aalto University publication series DOCTORAL DISSERTATIONS 193/2015

Field of research Neuroscience

Manuscript submitted 5 August 2015 **Date of the defence** 16 December 2015

Permission to publish granted (date) 27 October 2015 **Language** English

☐ **Monograph** ☒ **Article dissertation (summary + original articles)**

Abstract

The mammalian visual system is a dynamic and efficient data processing framework. Specifically, the cerebral cortex which is a structured network of cells benefits from an efficient information transmission coding. This thesis presents a model-based exploration of visual cortex in order to expand our current knowledge about brain mechanisms; specifically, the mechanism of information coding behind visual interactions.

In the first study, we designed a functional magnetic resonance imaging (fMRI) experiment to explore a possible link between contextual modulation and efficient macroscopic spatial response coding in the visual cortex. The results imply that visual interactions were best explained with a decorrelation model which predicts average modulation strength by fully decorating the spatial fMRI signals.

In the second study, we reviewed a potential approach to relate fMRI activation patterns to neural population activity. We went over existing knowledge about neurovascular coupling as a key point in predicting fMRI signal based on a neural network simulation and provided a sketch which covered practical steps to bridge the gap between mathematical modeling of single neuron responses to neuroimaging data with a mesoscopic biomimetic neural network. The proposed biomimetic neural network provides insight into data processing in cortical neural networks.

In the third study, we designed an fMRI experiment and based on the blueprint of the second study simulated a simplified neural network representing the visual cortex. Then, we tried to replicate the experimental fMRI signal by means of this biophysically plausible neural network simulator. Our results highlight the role of dendritic structure of neurons to be able to repeat the experimental fMRI signals with high fidelity.

In the fourth study, we used similar simulator as in the third study and tried to replicate expected neural activation pattern based on a well know contextual modulation (area summation function) in primary visual cortex. We anticipated that by getting closer to an activation pattern driven by area summation function, the efficiency of the neural network would be increased. Our results show that spiking frequency, entropy per spike and sparseness (as measures of network efficiency) are all associated with the natural area summation function.

In summary, results of this thesis suggest that contextual modulation is related to efficiency of the visual system. In addition, it is possible to predict fMRI and expected area summation activation pattern by a mesoscopic neural network, however compartmental neurons have a key role to achieve this prediction.

Keywords visual system, functional magnetic resonance imaging, efficiency, contextual modulation, spiking network model

ISBN (printed) 978-952-60-6529-8 **ISBN (pdf)** 978-952-60-6530-4

ISSN-L 1799-4934 **ISSN (printed)** 1799-4934 **ISSN (pdf)** 1799-4942

Location of publisher Helsinki **Location of printing** Helsinki **Year** 2015

Pages 62 **urn** http://urn.fi/URN:ISBN:978-952-60-6530-4

Acknowledgements

This PhD study was mainly accomplished in the Brain Research Unit, Department of Neuroscience and Biomedical Engineering, and AMI Centre, Aalto Neuroimaging at Aalto University. I thank Department of Clinical Neurosciences, Neurology at University of Helsinki and Helsinki University Hospital which supported the last year of this study. In addition, I would like to thank Academy of Finland, Finnish Graduate School of Neuroscience, Finnish Society of Sciences, Otto A. Malm foundation and Oskar Öflunds Stiftelse foundation for the financial supports.

I am grateful to my supervisor Prof. Matti Hämäläinen for his insightful comments and supports. In addition, I would like to thank Prof. Riitta Hari head of the BRU laboratory for her professional leadership which made this lab an excellent working environment. I thank my pre-examiners Doc. Teemu Rinne and Prof. Juha Voipio for reviewing my thesis and for their advantageous comments on the manuscript. Thanks to Prof. Simon Thorpe my opponent for accepting to attend my defence in Helsinki.

I am deeply grateful to my advisor Doc. Simo Vanni for his invaluable advises, continuous support, patience and kind encouragement. His scientific insight and striving for excellence influenced my scientific orientation and academic way of thinking most. Completing this thesis would not have been possible without his outstanding guidance and I couldn't have imagined having a better advisor along my way.

My sincere thanks also go to Prof. Lauri Nummenmaa, Doc. Ricardo Vigário, Dr. Hanna Heikkinen, Dr. Lauri Nurminen. I have learned a lot from all of you during our scientific collaborations. I thank Prof. Timo Erkinjuntti my supervisor and Prof. Synnöve Carlson my PhD follow-up group member at University of Helsinki. I am grateful to Doc. Juha Silvanto, Dr. Linda Henriksson and Dr. Toni Auranen for their advantageous comments on my work and Marita Kattelus for helping me with data collections. I would like to take a chance and thank all the former and current members of the BRU and AMI centre for the friendly company, helps, nice discussions, lunches etc. Specifically, I would like to thank Silvia, Mikko, Tuomas, Linda and Elyana.

My lovely mom and dad, I can never thank you enough for what you have done for me to reach my dreams. Thanks to my brothers Saeed and Reza for supporting me throughout all steps of my life. I also thank all my friends, especially my wonderful Iranian friends for creating a pleasant and warm atmosphere for me in Helsinki area. My dearest Ehsan, you are indeed my best friend, the one who made so many ordinary moments, extraordinary. Thank you for believing in me and your endless support at every moment of this PhD and for all the love you brought to our small family.

Espoo, 21 October 2015
Fariba Sharifian

Contents

List of Abbreviations and Symbols

ASF	Area Summation Function
BOLD	Blood Oxygenation Level Dependent
CBF	Cortical Blood Flow
DAS	Distance to Area Summation
EIF	Exponential Integrate-and-Fire
EPI	Echo Planar Imaging
fMRI	Functional Magnetic Resonance Imaging
HRF	Hemodynamic Response Function
hV4	Human V4
IF	Integrate-and-Firing
LFP	Local Field Potential
LGN	Lateral Geniculate Nucleus
MR	Magnetic Resonance
MRI	Magnetic Resonance Imaging
MSE	Mean Squared Error
MUA	Multi-Unit Activity
RF	Radio Frequency
TMS	Transcranial Magnetic Stimulation
TR	Repetition Time
V1	Primary visual cortex
VOI	Voxels Of Interest

List of Publications

This doctoral dissertation consists of a summary and of the following publications which are referred to in the text by their numerals

1. Sharifian F, Nurminen L, Vanni S (2013) Visual interactions conform to pattern decorrelation in multiple cortical areas. PLoS One 8(7): e68046. doi: 10.1371/journal.pone.0068046.

2. Vanni S, Sharifian F, Heikkinen H, Vigário R (2015) Modeling fMRI signals can provide insights into neural processing in the cerebral cortex. J Neurophysiol: jn.00332.2014. doi: 10.1152/jn.00332.2014.

3. Heikkinen H, Sharifian F, Vigário R, Vanni S (2015) Feedback to distal dendrites links fMRI signals to neural receptive fields in a spiking network model of the visual cortex. J Neurophysiol: jn.00169.2015. doi: 0.1152/jn.00169.2015.

4. Sharifian F, Heikkinen H, Vigário R, Vanni S (2015) Contextual modulation of receptive field increases efficiency in modelled visual cortex. Frontiers in Computational Neuroscience, under review.

Author's Contribution

Publication 1: Visual interactions conform to pattern decorrelation in multiple cortical areas

FS designed the experiments, measured and analyzed data, and had major contribution in writing the paper. LN contributed to interpretation of the results, helped in measurements and data analysis, and had major contribution in writing the paper. SV designed the experiments, consulted in data analysis, and had major contribution in writing the paper.

Publication 2: Modeling fMRI signals can provide insights into neural processing in the cerebral cortex

FS, SV, HH and RV wrote the review.

Publication 3: Feedback to distal dendrites links fMRI signals to neural receptive fields in a spiking network model of the visual cortex

FS designed and performed the fMRI experiment, participated in design and analysis of the neural network and writing the paper. HH designed, performed and analyzed the fMRI experiment, designed and implemented the spiking neural network, and had major contribution in writing the paper. RV analyzed data, designed model optimization and participated in writing the paper. SV initialized, designed, performed and analyzed the fMRI experiment, designed the neural network, and had major contribution in writing the paper.

Publication 4: Contextual modulation of receptive field increases efficiency in modelled visual cortex

FS designed, simulated, and analyzed the neural network and had major contribution in writing the paper. HH designed the neural network, and participated in writing the paper. RV participated in data analysis and writing the paper. SV designed and analyzed the neural network, and had major contribution in writing the paper.

1. Introduction

Anatomical and physiological studies of the mammalian brain show that the cerebral cortex is a structured network of cells. Specifically, in the visual cortex while stimuli are presented to this network of cells, the cells interact to produce the cortical activation. This interaction happens at multiple levels of cortical processing hierarchy. As a result of the neural interactions, the neural response to a specific stimulus is dependent on the context in which the stimulus is presented. This well-known phenomenon is called contextual modulation of neural responses. The network mechanisms behind contextual modulation have been accounted for using physiologically plausible models (Somers et al., 1998, Schwabe et al., 2006, Schwabe et al., 2010). For each cell, these models consider a large region of information access in the visual field via feedforward-feedback neural connections. In the primary visual cortex, contextual modulation has been associated with more efficient information transmission (Vinje and Gallant, 2000, 2002). In addition, there is some evidence that statistical dependencies between neural units are related to contextual modulation (Muller et al., 1999, Felsen et al., 2005).

In addition to the studies at the individual cell level, contextual modulation of macroscopic neural responses has been studied as well (Williams et al., 2003, Tajima et al., 2010, Vanni and Rosenström, 2011). However, some key questions about contextual modulation remain unsolved: (i) Similar to single-cell studies, can we expect an increase of neural network efficiency (see Section 1.3) at system-level as a result of contextual modulation? (ii) Is it possible to develop a computational neural network model to predict system-level cortical activations based on the single cell responses? (iii) Is it possible to identify the components of the neural network that have a key role in predicting the contextual modulation of responses? (iv) In the first question, we look for experimental system-level efficiency of contextual modulation, but can the computational neural network model quantitatively confirm the efficiency of contextual modulation?

In this thesis, we designed functional magnetic resonance imaging (fMRI, see Section 1.2) experiments to investigate whether the observed increase of efficiency in the single cell contextual modulation can be generalized to neuroimaging data. To address question (i), we explored how spatial correlations between cortical signals to center-and-surround stimuli are related to interac-

tions between the two cortical activations and studied such contextual effects in different visual areas and eccentricities (see Section 2.1). To answer question (ii), we reviewed the potentials and concerns of relating theoretical individual neural models (Hodgkin and Huxley, 1952, Fourcaud-Trocme et al., 2003, Burkitt, 2006b, Brunel and van Rossum, 2007) to macroscopic neuroimaging data (see Section 2.2). To tackle question (iii), we then developed a computational neural network and generalized the response of single neurons to a population of neurons in a neural network, in order to predict system-level activation patterns. We tried to optimize the open parameters of the model to best predict the fMRI and theoretical contextual modulation data. Therefore, we could investigate which parameters are more important in predicting the system-level contextual modulation responses (see Section 2.3). Finally, to confront question (iv) based on this neural network simulation, we tried to find the link between area summation function (contextual modulation as reflected in single cell receptive field) and efficiency of the visual system neural responses (see Section 2.4).

1.1. The visual system

The visual system is an important part of central nervous system as more than 25% of the primate cerebral cortex is directly involved in visual system, and it has been studied more extensively than compared to any other sensory system.

1.1.1. The retina

The first component of the visual system, retina, is a neural network with light-sensitive receptor cells located in the inner surface of the eye (for a review see (Wassle and Boycott, 1991)). The visual processing starts by conversion of light into an electrical signal, phototransduction, accomplished by photoreceptors in the retina. In the human eye, rods and cones are the most important photoreceptors (Yau, 1994) with major difference in functionality (for a review see (Burns and Lamb, 2004)). First, there are about 20 times more rods than cones in the human retina. Second, rods are triggered by much lower levels of light than cones and thus in usual day-light conditions cones mediate our vision. In addition, rods are not sensitive to colors and are more widely distributed across the retina than cones. The second step of retinal processing happens in bipolar cells (for review see (Nelson and Kolb, 2004, Euler et al., 2014)), which send signals from either a cone or a rod to ganglion cells. However, some of the bipolar cells receive signals from horizontal cells or send the signals to amacrine cells. The horizontal and amacrine cells introduce lateral inhibition. The bipolar cells can be either on- or off-center cells which contain inhibitory or excitatory synaptic connections, respectively. Ganglion cells are the last building blocks of the retina, and are considered as the output neurons of the retina (for a review see (Martin and Grünert, 2004)). In general, ganglion cells transform current into spike frequency and have center

and surround receptive fields (Kuffler, 1953). Parasol and Midget cells with different morphology of their dendrite arbours are the main types of the ganglion cells. The spatial distribution of Parasol and Midget cells varies across the retinal eccentricity (Dacey, 1993, Field and Chichilnisky, 2007). In the initial stage, the information from the Midget and Parasol cells transmit by two separate pathways which are termed parvocellular and magnocellular pathways, respectively.

1.1.2. Lateral Geniculate Nucleus

Almost 90% of the output of the retina is passed to Lateral Geniculate Nucleus (LGN) in the thalamus (Callaway, 2005). The LGN neurons have center-and-surround receptive fields, which helps to keep the cells sensitive for a wide dynamic range by avoiding the saturation. The main pathways in LGN are the magnocellular and parvocellular pathways (for a review see (Lennie and Movshon, 2005)). The cells corresponding to parvocellular pathway have a small receptive field. They are sensitive to high spatial frequencies and have low contrast sensitivity. The cells corresponding to magnocellular pathway have low spatial resolution but high contrast sensitivity (Livingstone and Hubel, 1988, Kaplan, 2004). These pathways project to different layers of primary visual cortex (Livingstone and Hubel, 1988). The LGN receives several feedback connections (almost 95% of the LGN input) from the visual cortex, superior colliculus, pretectum, thalamic reticular nuclei, and local LGN interneurons. Therefore, it has been suggested that LGN has an important role in modulating the information flow to the cortex using these feedbacks (McAlonan et al., 2008, Saalmann and Kastner, 2009).

1.1.3. The Visual Cortex

The main part of visual processing happens in the visual cortex located primarily in the occipital lobe. The visual cortex is a structural network of neurons that communicate by lateral, feedforward and feedback connections. The circuitry in visual cortex is formed the by anatomical connections (such as synaptic connections) between neurons and neurotransmitter receptor (functional mediators) systems (Rivadulla et al., 2001).

The visual cortex consists of the striate cortex (primary visual cortex, V1), extrastriate cortex (V2, V3, V4 and V5) and more than 20 other different cortical areas. These visual areas are defined based on their architecture, connectivity, visual topography, and functional characteristics. There are different definitions of these areas because of individual variability.

1.1.4. The Primary Visual Cortex

The primary visual cortex (V1) is the first level in the cortical visual system hierarchy. Like many other cortical arease, it has columnar functional organization (group of neurons with almost similar receptive fields (Rakic, 2008)) and also comprises six layers, numbered as 1 to 6 from the pial surface of the cortex towards white matter. Each layer has a distinct set of characteristics, such as neural connectivity, cell types, and possibly different data processing roles. The primary visual cortex has a clear and continuous retinotopy (for a review see (Ringach, 2004)). This means that almost every point in the visual field can be directly mapped by a simple mathematical formula (Schwartz, 1994) to the V1 neurons. The V1 neurons are tuned for basic stimulus features such as orientation (Hubel and Wiesel, 1959, 1962, Campbell et al., 1966), spatial frequency (Campbell et al., 1969) and direction of motion (Hubel and Wiesel, 1959, 1968). The primary visual cortex provides a good platform for studies of cortical circuits and computational models as it can be easily stimulated and its physical location in the cortex makes considerable part of it accessible by multiple experimental methods.

In a feedforward flow: (i) V1 mainly receives visual input from LGN to its Layer 4. (ii) V1 also receives input from some other brain regions as well (Orban, 2008) to its Layer 4. (iii) V1 sends feedforward output mainly from Layer 2 and Layer 3 to higher visual areas (Felleman and Van Essen, 1991a). However, the feedforward input from LGN comprise only about 2% of synapses to V1 and most of the rest originate from the recurrent local synaptic circuitry (Markov et al., 2011). In addition to the feedforward connection, V1 receives feedback mostly to its superficial layers from higher visual areas and sends feedback to LGN and thalamic reticular nucleus (Reich et al., 2001, Alitto and Usrey, 2003).

1.1.5. Other visual cortical areas

In addition to V1, V2 and V3 are also categorized as lower-order cortical areas as they are involved in processing of low-level visual features (Grill-Spector and Malach, 2004). V2 and V3 comprise two asymmetric, physically separated subdivisions. These sub-regions are named dorsal V2 and ventral V2, and dorsal V3 and ventral V3, respectively. In general, in addition to some similarities to V1, V2 and V3 neurons are also modulated by more complex visual characteristics of the stimuli (Van Essen et al., 1986, Boynton and Hegde, 2004). Higher-order visual areas include a large number of cortical regions (such as V4, V5, V6 and etc.). They are usually involved in more advanced data processing than lower-order cortical areas, such as motion and attention-controlled processing, for a review see (Orban, 2008).

1.1.6. Visual processing in the cortex

The structure and connections between different visual areas can be categorized into parallel processing streams, for a review see (Ungerleider and Haxby, 1994), or hierarchical processing (Felleman and Van Essen, 1991b, Barone et al., 2000). In parallel processing categorization (Figure 1.1a) the visual system transmits information to ventral or dorsal stream. Both streams start from primary visual cortex and pass through V2, then the ventral stream continues to V4 and inferior temporal cortex and is mostly associated with object recognition (Ungerleider and Haxby, 1994). The dorsal stream, in turn, continues to dorsomedial area (V6), MT / V5 visual area and the posterior parietal cortex, and is mostly associated with spatial or motion vision and attention. However, both streams are dynamic and may contribute to decoding and processing of visual features usually associated with the other pathway.

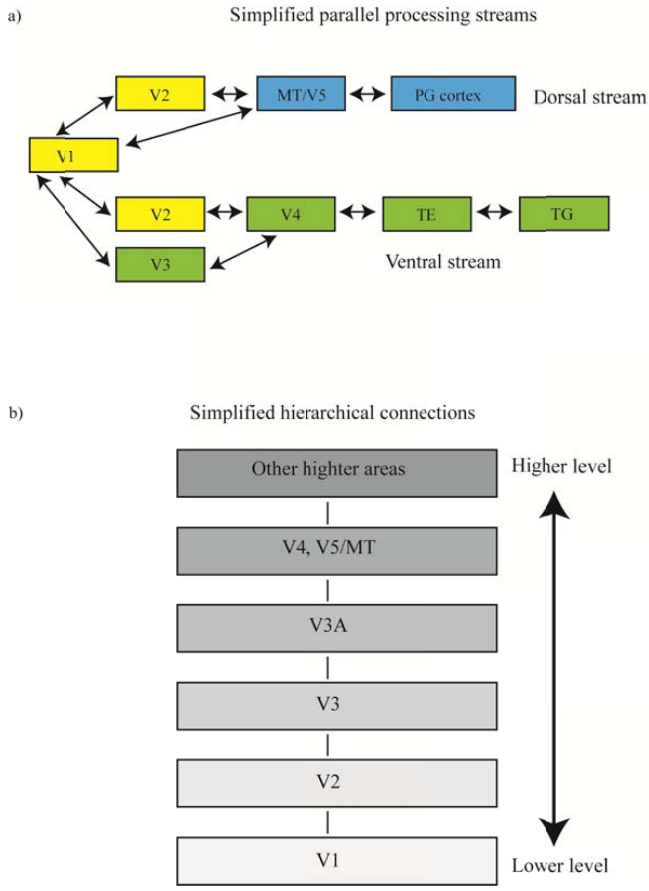

Figure 1.1. Two categorizations of the visual system processing. a) Simplified parallel processing streams and b) simplified hierarchical processing.

The hierarchical categorization shown in Figure 1.1b mostly considers the anatomical feedforward and feedback connections between visual areas. There is a large heterogeneity in these anatomical connection weights which has an

important role in understanding the visual cortical processing. For example, there is a very minor subcortical input, high local connectivity and low long-range corticocortical connectivity (Markov et al., 2011).

1.2. fMRI

Electrophysiological, optical, and anatomical in vitro methods are common ways to study animal brains. While these methods provide good spatial and temporal resolutions, they are invasive and offer limited possibilities to access multiple brain areas simultaneously. Functional Magnetic Resonance Imaging (fMRI) is a noninvasive imaging method which has a very high spatial resolution, while its temporal resolution is limited by the sluggish hemodynamic response. The hemodynamic fMRI signal has an indirect and complex association to actual neural activity through neurovascular coupling (for a review see (Huettel et al., 2004)).

1.2.1. Principles of MRI

In most medical applications of Magnetic Resonance Imaging (MRI) an image of the tissue is created based on a signal related to the protons in the water molecules. The protons have a property called nuclear spin and an associated magnetic moment which usually is oriented randomly. An MRI device provides both a strong and uniform magnetic field (B0 field, typically between 1.5-7 T), fields oscillating at radio frequencies (RF field), as well as magnetic field gradients. In the B0 field the nuclear magnetic moments form a net magnetization vector which orients itself to the direction of the B0 field and precess around the direction of the field with a specific frequency. This precession frequency is the frequency in which nuclear magnetic moment can efficiently absorb energy. This resonance frequency in rad/s is proportional to the B_0 field: $\omega = \gamma B_0$, where the nucleus-specific constant proportionality is called the gyromagnetic ratio. For a proton $\gamma/2\pi = 42.576$ MHz/T (Huettel et al., 2004).

Next, to create the Magnetic Resonance (MR) signal, a brief RF pulse is applied. The RF pulse oscillates at the precession frequency to provide efficient absorb of energy. This pulse turns the net magnetic moment away from the direction of B_0. As a result, the longitudinal component of the net magnetization decreases, and in addition, the RF pulse introduces a measurable transverse component to the net magnetization (MR signal). When the RF field is switched off the magnetic moments relax back original state and emit energy that can be detected as an RF signal. There are two time constants involved in the two simultaneous relaxation processes. The T1 relaxation time describes the rate the longitudinal magnetization is recovered while T2 relaxation is related to the decay of the transverse magnetization.

As mentioned before, the resonance frequency is proportional to magnetic field, which provides a basis for spatial encoding in MRI. This signal encoding is done with three spatially orthogonal magnetic field gradients. A specific slice is selected by applying a linear magnetic field gradient, and then, two orthogonal magnetic field gradients are used to encode spatial locations within one slice. The frequency and bandwidth of the RF pulse together with strength of the gradient magnetic fields determine the spatial resolution and encoding of the location (Huettel et al., 2004).

1.2.2. Functional MRI

The most common signal used in fMRI originates from the difference in magnetic properties of deoxygenated and oxygenated hemoglobin. Deoxygenated hemoglobin is paramagnetic whereas oxygenated hemoglobin is diamagnetic. Therefore, decreased density of deoxyhemoglobin causes an increase of MR signal. This fMRI method is called Blood Oxygen Level Dependent (BOLD) contrast imaging (Ogawa et al., 1990). In the brain, higher neural activity in a specific region usually associates with increased amount of oxygen consumption and consequently increased Cortical Blood Flow (CBF) to provide energy to the neurons by glucose oxidation (Raichle and Mintun, 2006) in that region. More specifically, active neurons release neurotransmitters during neural activity. Astrocytes recycle these neurotransmitters back to the neurons. The blood flow appears to be directly linked with the signaling between active neurons and astrocytes. For a review, see (Haydon and Carmignoto, 2006).

The BOLD signal emerges from a combination of three factors: (i) oxygen consumption which locally increases deoxyhemoglobin resulting in reduction of the BOLD signal. (ii) The change in cerebral blood flow which is more than the oxygen consumption and cause reduction of deoxygenated hemoglobin. Thus, it results in positive BOLD signal. (iii) The change in cerebral blood volume due to increase of the blood flow and vessel wall capacitance in the small veins which cause increase in deoxyhemoglobin concentration and subsequently non-linearly decrease of the BOLD signal. In addition, earlier studies show that positive BOLD signal is correlated with both the Multi-Unit Activity (MUA) and the Local Field Potentials (LFP), and the LFP seems to be better linked to the BOLD than MUA (Magri et al., 2011).

Due to slow blood flow response, BOLD signal shows a temporal dynamic. This temporal dynamic is termed Hemodynamic Response Function (HRF). After neural activation the signal starts to increase from its baseline about 2 s after the stimulus onset. Next, the BOLD signal rises to its maximum level about five seconds from the start of stimulus. Later, signal drops quickly a bit under its baseline and then returns to the baseline almost after 16 s from the stimulus onset (Figure 1.2). Many studies have also reported an initial dip

before the increase of signal and tried to use it for providing a better link be-between neurovascular coupling and neural activity (Hu and Yacoub, 2012). However, there is individual variability in the measured HRF as well (Aguirre et al., 1998).

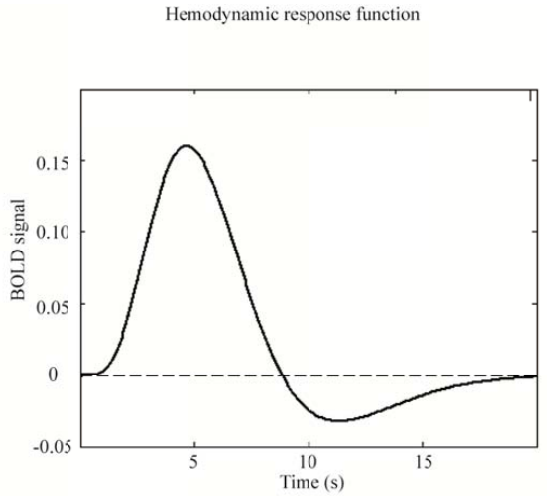

Figure 1.2. Hemodynamic response function. Dashed line shows the baseline.

1.2.3. fMRI as a brain research tool11

fMRI has several applications. In some studies the aim is to establish a functional map of the cortex, i.e., to relate activated cortical areas to a given stimulus. With present fMRI methods a resolution of 1 mm^3 is achievable (although 2 mm^3 is a more typical resolution). However, BOLD fMRI might have the potential of increasing the spatial resolution even to the level of a single cortical column (Logothetis, 2008). A cortical column may refer to anatomical or functional columnarity, which could be defined based on different neural properties (Rakic, 2008). Functional column is defined as a group of about 10^4 neighboring neurons with similar tuning properties. This number of neurons usually covers 0.3-0.4 mm^2 of the cortical surface and represents a functional unit, with particular connectivity to other columns (Mountcastle, 1997). To achieve the resolution of a single cortical column, an ultra-high field MRI scanner, a large number of receiving coil elements, and parallel excitation are probably necessary (Logothetis, 2008).

Recent fMRI studies (Goense and Logothetis, 2006, Ress et al., 2007, Koopmans et al., 2010, Polimeni et al., 2010, Goense et al., 2012) have been able to separate activation strengths at three different laminar depths: supragranular, granular and infragranular, corresponding roughly to layers 1-3, 4 and 5-6 respectively. This spatial resolution provides the opportunity to study intra-cortical functional organization. However, further technical development is necessary to be able to segregate all cortical layers.

1.2.4. fMRI challenges

The baseline concentration of deoxyhemoglobin depends on many factors. For example, different brain areas, individuals and physiological states result in varying deoxyhemoglobin concentration. To address this problem, usually the mean signal is subtracted in fMRI analysis. Another problem is that density of vasculature varies between cortical areas which affects the BOLD signal change as a function of neural activity (Reina-De La Torre et al., 1998). To overcome this problem, when comparing different brain areas arterial spin labelling technique (which allows the weighting of the MRI signal by cerebral blood flow) provide a better estimate of the absolute value of blood flow changes compared to direct compare of the signal (Calamante et al., 1999).

One of the most important challenges of interpreting the fMRI signal arises in studies interested in the quantity of BOLD signal. Specifically, in case of having negative BOLD signal, it is important to know to what extent the BOLD signal nonlinearities might be explained by hemodynamic redistribution of blood known as vascular stealing. Systematic changes in visual parameters showed that the nonlinearity has a strong neural origin (Pihlaja et al., 2008). In addition, negative BOLD response has been associated with reduction of neural activity (Shmuel et al., 2006, Boorman et al., 2010) and cerebral metabolic rate of oxygen consumption (Devor et al., 2005, Pasley et al., 2007). Moreover, hyperpolarization of the neuronal membrane potential has been correlated with negative BOLD signal (Devor et al., 2007). These findings confirm that the blood stealing cannot explain the reduction of BOLD signal during negative BOLD response. In addition, the positive and negative BOLD responses show different behavior in increase and decrease of cortical blood flow and volume in different cortical layers. This suggests distinct mechanisms of neurovascular coupling for positive and negative BOLD responses (Goense et al., 2012).

Another important challenge in fMRI studies is dealing with the noise caused by the head motion (Friston et al., 1996, Andersson et al., 2001). The most common anatomical procedure to deal with this problem is the co-registration of the functional volumes to a reference volume. However, due to interactions between the head movement and head-induced inhomogeneity of the magnetic field, residual motion-related variance may still remain (Andersson et al., 2001). Therefore, estimation of the motion parameters from the co-registration and using the in signal analysis might help to exclude the residual variance.

1.3. Efficiency in a network

The brain, as a network of interconnected neurons, is very efficient in

processing of natural data. In a neural network, one measure of efficiency is coding efficiency. The amount of information that can be transmitted with one unit of energy could be defined as coding efficiency. Reduction of redundancy in a response output of a neural network has been linked to coding efficacy (Barlow, 1961, Barlow and Földiak, 1989) as it increases the efficiency of information transmission. In addition, sparse coding can increase network coding efficiency. Sparsely coded network is usually defined as a pattern in which a small fraction of the neurons encode the signal and the rest remain relatively silent.

In a natural environment, input data (for example visual stimulus) contains a set of statistical dependencies delivered to the sensory information flow. For a statistically optimized representation of the sensory information brain works as a multivariate system. In this multivariate system a set of basis functions provide learning by simplifying and sampling new sensory inputs (Rao and Ballard, 1999). This means that in the process of learning the error between the input and the learned basis vector is propagated to the next hierarchical level and the prediction based on the basis vectors is back propagated to the previous hierarchical level. Based on the information theory, to achieve the largest capacity of information transmission with given number of units, a message should comprise equal probability of activation in each unit (Shannon, 1948). In the learning process redundant data is important until it signals to higher order structure of network and updates the basis functions. After that adaptation to these statistical regularities is important to avoid redundancy and have an efficient sensory signal processing (Field, 1987, Rao and Ballard, 1999, Simoncelli and Olshausen, 2001, Friston, 2010).

It has been suggested that coding efficacy is achieved with decorrelation of correlated neural responses (Barlow and Földiak, 1989). If neural patterns are independent, they are necessarily also uncorrelated. Therefore, decorrelation might be a valid substitute for independence in neural networks. However, decorrelation might be a separate process from the sparse and independent coding, although it is a common preprocessing step in computational algorithms which aim to find sparse and independent components (Olshausen and Field, 1996, Hyvärinen et al., 2009).

There are two types or correlation in neural responses: (i) Noise correlations, indicating the dependencies between trial-to-trial variability of neural responses. This means that for each stimulus the population activities are correlated. (ii) Signal correlations, which is the relationship between mean firing rates across of neurons with similar tuning functions. For example, cells with overlapping receptive fields produce signal-correlated outputs. To reduce signal correlations, it is not efficient to learn regularities during one sensory event and have a fixed structure for decorrelation because each sensory event has particular dependencies which cause new correlations in the spatial activation patterns. Therefore to maximize information transmission capacity,

it is necessary to have a neural code which rapidly adapts to the statistics of the sensory environment (Laughlin, 1981, Muller et al., 1999, Brenner et al., 2000, Fairhall et al., 2001, Vinje and Gallant, 2002, Sharpee et al., 2006). This adaptation can happen for example by shifting in the sensitivity of a neuron according to continuous stimuli in time or place. This has been shown both for low-level parameters in simple systems, such as contrast in insect compound eye (Laughlin, 1981), and also for more complex regularities in complex systems, such as orientation tuning in mammalian primary visual cortex (Gilbert and Wiesel, 1990, Muller et al., 1999, Felsen et al., 2005).

Recent studies suggest that even the macroscopic activation patterns carry significant information about underlying neural network (Haxby et al., 2001, Kay et al., 2008, Mitchell et al., 2008). Moreover, the information in macroscopic activation patterns has been successfully used for multivariate pattern classification and prediction of the activation patterns. Therefore, efficiency of a neural network is expected to be accessible already in the macroscopic (for example fMRI) population activity and not only at local intravoxel population.

1.4. Neural interaction models

1.4.1. Contextual modulation

In the visual system, the neural response to a separately presented visual stimulus might not be equal to the neural response to that stimulus, while it is surrounded with another stimulus: the response to a stimulus depends on the context in which it is presented. This well-known phenomenon is named contextual modulation. Contextual modulation suggests that local and feedback information (Angelucci et al., 2002), or even information from other sources than visual sensory system affect the processing of a given stimulus. Contextual modulation has been observed and studied in different levels of the visual system using several methods, for example in behavioral (Cannon and Fullenkamp, 1993, Xing and Heeger, 2001, Nurminen et al., 2010), single neuron (Levitt and Lund, 1997, Ichida et al., 2007), and system-level (Williams et al., 2003, McDonald et al., 2009, Wade and Rowland, 2010, Vanni and Rosenstrom, 2011). In general, context can reduce or increase the neural response; the former is called suppression and the latter facilitation, respectively.

At the single-cell level, contextual modulation has been widely studied in both spatial and temporal (for example, adaptation) dimensions. From intracellular properties of neurons, we know that despite sharp input tuning of the action potential, output of a single neuron is affected with very distant stimuli. Specifically, spatial contextual modulation of V1 neurons suggests that surround stimulus outside the classical receptive field can non-linearly

modulate responses of V1 neurons. Usually, stimulation of the extra-classical receptive field reduce firing rate evoked by stimulus inside the classical receptive field (Solomon et al., 2006). However, increase of the firing rate could be expected as well (Levitt and Lund, 1997, Ichida et al., 2007). In spatial contextual modulation the level of interaction is affected by the surround distance: the closer stimuli usually have a stronger modulation effect (Cannon and Fullenkamp, 1991, Levitt and Lund, 2002). In addition, the contextual interactions are affected by spatial frequency and orientation differences between the center and surround stimuli. Usually, having the center and surround at the same spatiotemporal frequency (Webb et al., 2005) or orientation (Cavanaugh et al., 2002) leads to a very strong modulation. In addition, in most of the cases surround in relation to center stimuli contrast is an important factor in determining the modulation strength. Usually, higher contrast of surround leads to suppressive effect (Chubb et al., 1989, Snowden and Hammett, 1998, Olzak and Laurinen, 1999). Contrast facilitation is sometimes observed when the surround has a lower contrast than the center (Xing and Heeger, 2001).

Many theoretical and experimental studies show that processing and coding of sensory information is affected by the statistical regularities of the environment (Barlow, 1961, Olshausen and Field, 1996, Hyvärinen et al., 2009). Therefore, in addition to spatial contextual modulation, the neural response to visual stimuli might be modulated by non-spatial contexts such as attention, adaptation and learning.

Contextual modulation has been also reported in system-level studies (Williams et al., 2003, McDonald et al., 2009, Wade and Rowland, 2010). For example, in fMRI studies spatial context affects the BOLD responses in the early visual cortices of humans (Dumoulin and Hess, 2006). In addition to system-level spatial contextual modulation, early fMRI studies of temporal contextual modulation show that repeating the same stimulus leads to reduction of the BOLD signal (Grill-Spector et al., 1999, Grill-Spector and Malach, 2001).

Several experimental and theoretical studies aimed to model the network mechanisms behind contextual modulation with physiological models. Specifically, Schwabe et al. (2006) tried to explain how the excitation and inhibition are linked. They suggested a network of lateral, feedforward and feedback connections, to model contextual modulation with surround suppression and facilitation. In their model feedback comes from higher- to lower-order areas and excitatory feedback connections can suppress responses via inhibitory interneurons. In addition, another network model (Tsodyks et al., 1997) suggests that recurrent excitation and feedback inhibition are always present in the system and suppression is associated with withdrawal of recurrent excitation (Ozeki et al., 2009).

However, the models introduced above do not consider how visual system might benefit from contextual modulation and do not address the computational benefits of contextual modulation. A number of studies have suggested that contextual modulation is associated with decorrelation of correlated neural activation (Vinje and Gallant, 2000, 2002, Felsen et al., 2005). This decorrelation is linked to coding efficiency of visual information. In addition, sensory environment contains statistical regularities. Adaptation to such regularities is important for efficient coding without loss on information by suppressing the noise correlation effect, for a review see (Averbeck et al., 2006).

1.4.2. Area Summation

For a neuron located in primary visual cortex, the classical receptive field (center) threshold for driving action potentials is very low. However, in the extra-classical receptive field which is surrounding the classical receptive field, the stimulation does not drive action potentials directly but modulate the response of the neuron. In the primary visual cortex contextual modulation has been studied very systematically. This means, the response of a neuron has been quantified by a size-varying circular grating stimulus centered at the neuron's receptive fields. In this case, most of neurons show a non-monotonic response as a function of stimulus size (Sceniak et al., 1999, Angelucci et al., 2002, Cavanaugh et al., 2002). This non-monotonic response curve, Area Summation Function (ASF), starts with a sharp increase to a peak in neural firing rate, when the size of the stimulus increases. Once the stimulus diameter exceeds a certain level, called grating summation field, the response begins to drop until reaching an asymptote (Figure 1.3).

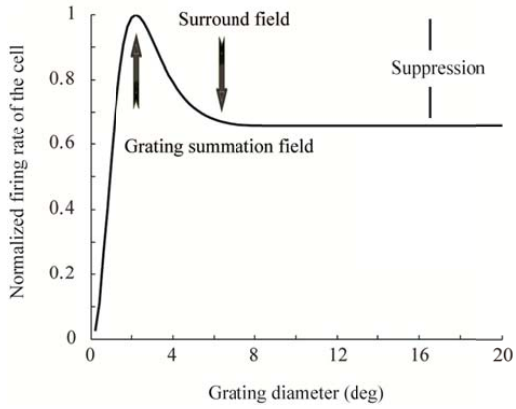

Figure 1.3. Area summation function. The function shows the schematic summation field size, and suppression strength, for a V1 neuron.

The spatial structure of the classical and extra classical receptive field has been modeled with two opposite Gaussian functions (Cavanaugh et al., 2002). The

shapes of the area summation function, and correspondingly, these Gaussian functions, are dependent on the stimulus parameters in the classical and extra-classical receptive field. For example, relative orientation or contrast of center and surround modulate the shape of the ASF (Knierim and van Essen, 1992, Levitt and Lund, 1997). However, previous studies of ASF do not mention why such non-linear area summation is useful for biological visual signal processing. For example, it is not known how this non-linear ASF could be related to an improvement of visual system efficiency.

2. Specific studies

2.1. Study I: Visual interactions conform to pattern decorrelation in multiple cortical areas

Contextual modulation (see Section 1.4.1) is an extensively-studied, robust phenomenon (Maffei and Fiorentini, 1976, Gulyas et al., 1987, Knierim and van Essen, 1992, Levitt and Lund, 1997, Sceniak et al., 1999, Li et al., 2000, Angelucci et al., 2002, Cavanaugh et al., 2002, Felsen et al., 2005, Ichida et al., 2007) which affects dependencies between neurons (Muller et al., 1999, Felsen et al., 2005) and has been associated with efficient information transmission in the primary visual cortex (Vinje and Gallant, 2000, 2002). Recent work (Vanni and Rosenstrom, 2011) suggested that contextual modulation relates to decorrelation, and interaction in functional magnetic resonance imaging data can be modeled with a simple cortical decorrelation model. They proposed that the average suppression and facilitation of the activation pattern nonlinearly links to decorrelation of the mean responses. Such decorrelation would cause reduction in redundant responses across cerebral cortex. This in practice cause independence in statistical properties of the activation patterns for two different stimuli.

In this study, we designed an fMRI experiment to explore how BOLD signal strength, sign, and spread in the visual cortex are associated with contextual suppression and facilitation. In particular, we studied how the correlation between spatial activation patterns of visual stimuli is related to average contextual modulation across voxel population in different parts of the visual cortex. In other words, in spatial domain, we studied how similarities of the mean blood oxygenation level dependent signal between cortical responses are related to suppression and facilitation. We investigated contextual modulation with different eccentricities of the stimuli in different visual cortical areas.

2.1.1. Methods

We studied fifteen adult subjects (age 20-44 years, 12 males), with normal or corrected-to-normal vision. The subjects were presented with five different stimuli with sinusoidal pattern and 0.5 c/deg spatial frequencies. Center, near and far surround stimuli were presented sequentially, or simultaneously (Figure 2.1). The contrast of the stimuli was 15%, with 40 cd/m2 mean display luminance. All the stimuli were generated with Matlab™ (Mathworks, Natick,

MA, USA) and we used Presentation™ software (Neurobehavioral Systems, Albany, CA, USA) to control the timing and positioning of the stimuli. The subjects viewed the stimulus at 34-cm distance via a surface mirror in front of their eyes. The order of the stimuli was pseudo-random and subjects were engaged in an attention controlling task during the stimulation.

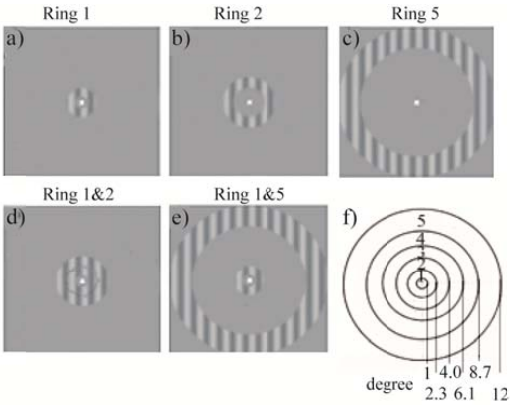

Figure 2.1. The main experiment comprised five different stimuli (a–e): a) Center (C, Ring1) alone, b) near surround (S_N, Ring2) alone c) far surround (S_F, Ring 5) alone d) center and near surround and e) center and far surround. The contrast of stimuli in this figure is higher than in the actual stimuli (15%). f) Eccentricity of the borders of the rings. The functional localizer for eccentricity representation comprised all five rings in a multifocal design.

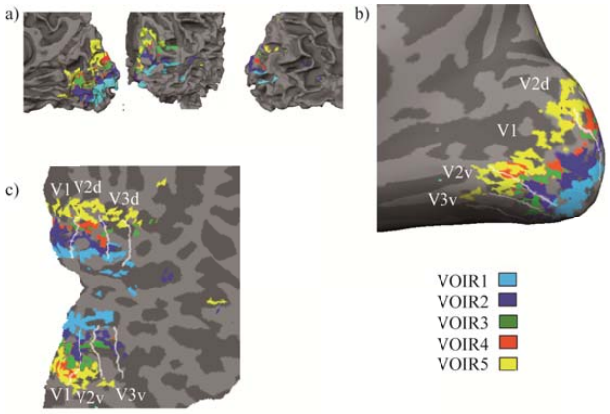

Figure 2.2. Activation for the five different rings in the multifocal localizer for one subject (S3). T-threshold was P_{FWE}=0.05. a) Activation on segmented white-matter/gray-matter border from three different angles, medial, posterior and lateral, respectively. b) Inflated right hemisphere surface, with different retinotopic areas separated by white lines. c) Unfolded view. The VOI_{R1-R5} indicate the voxels-of-interest for ring 1 to 5 (displayed in Figure 2.1) measured with the multifocal functional localizer.

We used General Electric Signa HDxt 3.0 T MRI (General Electric Medical System, Milwaukee, WI, USA) device. The RF head-coil had 8 phased-array

channels. The acquisition volume consisted of a 64*64 matrix, covering 18 cm field of view, and 29 slices, with 2.8 mm thickness. For each subject, we ran five Echo Planar Imaging (EPI) acquisitions with 30 ms echo time, and 60 degrees flip angle. Each acquisition had 158 time points with Repetition Time (TR) = 1.8 s. In addition, we had a functional localizer acquisition with similar acquisition parameters, but 164 time points. All subjects also participated in a separate fMRI session for mapping of lower-order retinotopic areas (Henriksson et al., 2012), ventral stream areas and V5. The cortical mapping together with functional localizer run could localize the active areas by each stimuli ring in different cortical areas (Figure 2.2).

After data collection, the fMRI data were preprocessed by converting them to NIFTI format, slice time correction, and realignment with reslicing (Friston et al., 2007). We followed the standard segmentation procedure, and an expert evaluated the quality of segmentation of each subject during and after the segmentation.

We defined the functional response in visual cortex to presenting center alone as C, and surround alone as S (SN: Near surround and SF: Far surround). While both center and surround stimuli are presented simultaneously, we assumed that the component responses become decorrelated, and denoted the decorrelated response for center as C', and that for surround as S', respectively. Naturally, C' and S' cannot be measured separately, but we can only measure their sum, which is denoted m(C,S), a measured function of original component responses. We assumed a linear summation of the components: m(C,S) = C'+S' . If C is larger than C', surround suppressed the center and if C is smaller than C', surround caused facilitation in the center. The same applies to S, respectively.

We defined d for each voxel as a suppression index of contextual modulation, d might be theoretical d (d_T, defined later) or measured d (d_M):

$$d_M = 1 - m(C,S) / (C + S) \qquad (2.1)$$

We know the C, S, and m(C,S) responses from the fMRI measurement for each voxel and could thus compute d_M for each voxel separately.

Next, d_M was compared to a d-value which would optimally decorrelate the vectors C and S. Vanni and Rosenstrom (2011) showed that C' and S' become fully decorrelated by a simple function of C, S and d:

$$\begin{aligned} C' &= C - d * S \\ S' &= S - d * C \end{aligned} \qquad (2.2)$$

This was done as follow: First, a vector of BOLD responses for C and S stimuli in a single set of Voxels Of Interest (VOI) were placed in Equation 2.2. Next,

with appropriate selection of a scalar d-coefficient for all the voxels, Equation 2.2 can fully decorrelate the two vectors (Vanni and Rosenstrom, 2011). Here, the d is a real number between -1 and 1. The appropriate fully decorrelating, d-coefficient was termed theoretical d-coefficient (d_T), and was calculated from the spatial correlation of voxel activation patterns C and S. While calculating d_T, we set zero covariance between C' and S' and then d_T came as a root of a quadratic equation. After solving Equation 2.2 for d, we had fully decorrelating d-coefficient (d_T) (see (Vanni and Rosenstrom, 2011) Supplementary equations for details). This d_T was compared to mean of voxel-wise determined d_M across the same voxel population.

2.1.2. Results

Subtracting C+S, from m(C,S) show that the activation for simultaneous presentation of C and S is not a linear sum of the components (Figure 2.3). The result of this subtraction can be either positive or negative, which indicate suppression and facilitation of center activation, respectively. Our results show that, in V1, V2 and V3, the near surround clearly caused more suppression than the far surround (Kolmogorov-Smirnov test, $p < 0.005$).

In addition, we analyzed how correlation between center and surround mean response patterns relates to suppression and facilitation. For both near and far surround, Figure 2.4 shows the average measured d-coefficient (d_M, mean suppression index across voxels, Equation 2.1), against signal correlation (C,S). Each point indicates average d_M of active voxels within VOIc (which includes voxels which are active for center stimuli), for one subject. The mean d-coefficient for each subject clusters close to the prediction (d_T, solid curve), for both near and far surround conditions. In line with the cortical decorrelation model (Vanni, 2012) both near and far surround conditions show that suppression strength is linked to signal correlation between responses.

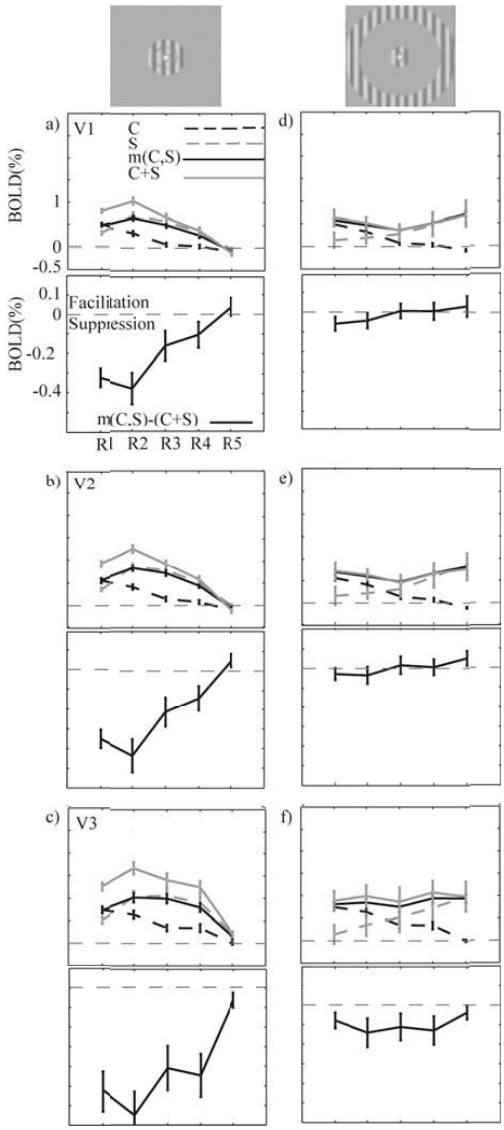

Figure 2.3. The group mean BOLD signal changes (%) as a function of eccentricity. The C, S, m(C,S) and C + S signals, for V1, V2 and V3 areas, are plotted separately for near surround (a–c) and far surround (d–f) conditions. The lower panel of each graph shows the subtraction m(C,S) – (C + S) revealing suppressive interaction or facilitative interaction amplitude. Voxel selection was thresholded at $P_{FWE} = 0.05$. Error bars display the standard errors of the means across the subjects. Note that the data for C is the same in the left and right columns.

Moreover, we show that visual stimulus can modulate the BOLD signal far from the stimuli response retinotopic position in V1-V3 (which shows the strongest responses), and that the sign of BOLD signal changes is linked to suppression and facilitation. The positive BOLD signals are consistently surrounded by negative BOLD signals in voxels which are further away from the strongest activation. In addition, far surround evokes facilitation of BOLD responses, especially in the voxels where either the mean C or S or both

responses are close to zero or negative (V1 and V2). Moreover, our results show that higher-order retinotopic areas have more suppression than the lower-order areas, for both near and far surround; and suppression was stronger in near than far surround (post-hoc test based on ANOVA, $p<0.05$).

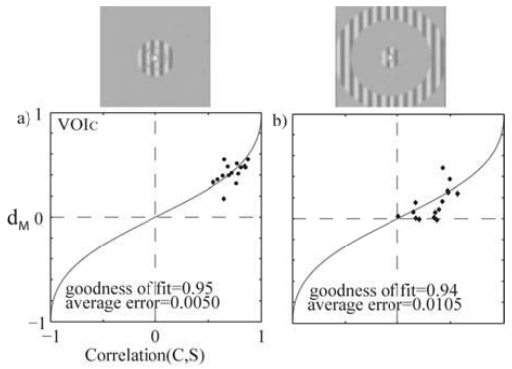

Figure 2.4. Correlation between C and S vectors versus average d_M, for 15 subjects. The results for the a) near and b) far surround conditions, respectively. for voxels of interest of center stimuli (VOI_C) at $P_{FWE} < 0.01$. The error bars show standard error of mean for average error across all subjects (data points).

In summary, our results show that regardless of the area selection, high correlation between center and surround mean responses was associated with stronger suppression. Context induced both suppression and facilitation far from the maximum retinotopic response. In addition, different signs of center and surround blood oxygenation level dependent signal was linked to facilitation, and the same signs to suppression. This is in line with cortical decorrelation model (Vanni and Rosenstrom, 2011) that suggest facilitation emerge from negative signal correlation. The wide cortical spread of the sub-threshold blood oxygenation level dependent signal indicates that for any visual stimuli changes in synaptic activity takes place in a surprisingly large network. This study provides further support for the cortical decorrelation model (Vanni, 2012) and suggests that global spatial interactions among neural populations emerge from ubiquitous application of the same decorrelation principle.

2.2. Study II: Simulating fMRI signals can provide insights to neural processing in the cerebral cortex

Computational models help to understand information processing in the brain. Theoretical neuroscience studies have yielded mathematical models of single neuron function (Hodgkin and Huxley, 1952, Fourcaud-Trocme et al., 2003, Burkitt, 2006b, Brunel and van Rossum, 2007) and have made it possible to simulate a single neuron and network responses (for review see (Sejnowski et al., 1988, Arbib, 2003)). The knowledge about single neuron functionality has led to mesoscopic models which can provide systems-level simulations of neuronal populations. Usually, these mesoscopic models

predict the probability distributions of neural firing rates and avoid detailed simulations of single neurons (for review see (Deco et al., 2008, Pinotsis and Friston, 2011)). By avoiding the details, but keeping the essential features, mesoscopic models reduce the computational costs compared to simulation of every single neuron. In addition, the number of more effective parameters decreases by a huge factor compared to detailed models. A comprehensive mesoscopic model of the cortex has the potential for many applications in both basic and clinical neurosciences. In addition, it might significantly increase our understanding of biological information processing.

In this review, we analyzed the requirements for providing a mesoscopic biomimetic models which enable system-level simulations of neural mass action on the basis of fMRI data. We used the neural network term for this mesoscopic biomimetic model of neural population.

2.2.1. Functional magnetic resonance imaging complements electrophysiology

To understand the functions of a cortical area, *e.g.*, the primary visual cortex (Olshausen and Field, 1996), it is necessary to have a fair sample of all types of neurons in different cortical layers. In addition, it is crucial to have access to the responses of all these neurons simultaneously. This makes it possible to come up with a realistic prediction of the population response.

A lot of the information about the structure and function of neural systems comes from cellular, anatomical and physiological studies. However, many of the methods employed in these studies lack the ability to monitor the activities of a very large ensemble of neurons. Macroscopic imaging methods like fMRI have the ability to sample the aggregate response of all types of neuron at the same time. However, studies aiming at proper understanding of neural function generally require methods with better spatial resolutions than fMRI. Furthermore, fMRI is not sensitive to the data processing inside a neuron. Information about single cell processing is necessary as this processing affects the input signals before they reach the axon's initial segment (Poirazi et al., 2003, Sidiropoulou et al., 2006, Jia et al., 2010). Moreover, the fMRI response is an indirect measure of the neural activity and can only sample neural activation coupled to vascular responses. Therefore, fMRI can complement but not replace anatomical and physiological data.

2.2.2. Bridging neural activation to fMRI data

The first issue to bridge the neural-level activation to fMRI signal is to find a proper biological model for the neurons located in the computational neural network. All these neurons need to be distributed on a realistic location. Next, the neurons need to interact to each other by different types of connections. By

existing technology, it is almost impossible to have a computational neural network comparable to the size of realistic neural network. Therefore, it is necessary to come up with a computationally feasible scale of the network to be able to do the simulation. Finally, this computational neural network needs to be evaluated in respect to measured BOLD signals.

Biophysical Models of Neurons

Biological neural models provide mathematical explanation of signal processing in neural-level. The important factors to choose a proper biological neuron model are: (i) robustness of the model (this means that small errors in initial parameter assignment should not ruin the functionality of the model), and (ii) efficiency (as in a computational neural network there are huge amount of neurons).

The most popular and well-known biological neuron model is integrate-and-firing (IF) model (based on Lapique's work 1907, translated in (Brunel and van Rossum, 2007) and for a review see also (Burkitt, 2006a)). However, this early IF model was not complete and failed in reflecting the physiological reality. Later, many other extensions of the IF model were introduced (for a review see (Burkitt, 2006a)) to make the model more accurate and try to describe different types of neurons.

Extended versions of IF model have the ability to reasonably predict the output of a single neuron. However, while vast number of studies reported the complex and diverse roles of information processing within dendritic structures (Spruston et al., 1994, Poirazi et al., 2003, Polsky et al., 2004, Sidiropoulou et al., 2006, Sjöstrom et al., 2008, Spruston, 2008, Gollo et al., 2009, Branco and Hausser, 2010), it is customary to make gross simplifications when constructing larger scale network models by considers a neuron as a single compartment. In addition, as it has been explained in Section 1.2, fMRI signal associates best with input of neurons. Therefore, in a computational neural network which aims to predict the BOLD signal, we would need to extend the IF model to include the difference between neural inputs and outputs.

In summary, the IF models are computationally cheap and have the capability to be upgraded in order to include dendritic dynamic. In addition, the IF model can be expanded to include multiple neuron types in the network (Naud et al., 2008).

The neural network structure and interactions

In a computational neural network, the response of a single neuron in an isolated area is not interesting. Rather, the response of a neuron while communicating to a mass of neurons originates the output of the network. In such a neural network, the spatial position of each neuron, type and strength of the connections between the neurons makes the body of the network. In a

simplified neural network, the connections between the neurons could either be the connections between different neurons or the connections between different cortical areas (for review see (Deco et al., 2008, Pinotsis and Friston, 2011, Pinotsis et al., 2012)).

Neurons interact with inhibitory and excitatory synaptic connections. The human cortex contains approximately 3×10^{10} neurons, with a ratio of 20-80 between inhibitory and excitatory neurons (Nieuwenhuys, 1994). These inhibitory and excitatory neurons might have different distribution, types, connections, and even different number of inhibitory and excitatory synapses (Bernander et al., 1994, Megias et al., 2001) with different roles in cortical information processing. Inhibitory connections are necessary to have an efficient network. In a completely efficient neural network neurons are mutually independent and have identical response probability profiles (Shannon, 1948). However, the exact mechanism of these interactions is still unknown.

Simulation and evaluation of a computational neural network

About $1.5x10^8$ of the approximately 3×10^{10} neurons in the human brain belong to primary visual area in each hemisphere (Leuba and Kraftsik, 1994). This translates to almost 10^4 neurons in a 0.4 cm^2 of cortex. One way to decrease the complexity of the computational neural network is to simulate each cortical column with a single representative neuron. The number of neurons in the simulation thus becomes equal to the number of cortical columns in the simulated functional area. Another benefit of having columnar resolution is the compatibility with potential spatial resolution of fMRI, which can approach the size of a cortical column, see Section 1.2. However, this simplification leads to intra-columnar details getting lost and thus might result in underestimation of local connections roles.

In order to compare the response of the computational neural network to fMRI signal, it is necessary to take neurovascular coupling into account. From the neural network simulation, we would have the action potential frequency which can be averaged to yield simulated multiunit activity. As explained in Section 1.2, Magri et al. (2011) suggested a direct relationship between BOLD and MUA. In addition, fMRI signal has been reported to correspond better with LFP rather than action potentials (Logothetis et al., 2001, Nir et al., 2007). These suggest that the BOLD signal would primarily reflect synaptic signaling and thus neural input. In neurovascular coupling the role of astrocytes has recently been emphasized (Zonta et al., 2003, Koehler et al., 2009). This means that the fMRI signal can be explained by astrocytic signaling mechanisms (Lin et al., 2010).

Such a mesoscopic neural network, together with the theoretical basis of systems neuroscience, brings a very strong explanatory power and might help to have a better understanding of biological data processing. In addition, as

the mammalian brain is very efficient, and a mesoscopic neural network inspired by biology might suggest efficient information processing mechanisms with industrial applications.

2.3. Study III: Feedback to distal dendrites links blood oxygenation level dependent signals to neural receptive fields in a spiking network model of the visual cortex

In this study, we investigated the spatial extent of the BOLD responses in the primary visual cortex. In several studies, it has been reported that the BOLD responses spread over much longer distances (Zuiderbaan et al., 2012, Sharifian et al., 2013) than what the small receptive fields of individual neurons could predict (Cavanaugh et al., 2002). Although BOLD response and local neuronal activity in the brain are closely linked (Logothetis et al., 2001, Goense and Logothetis, 2008, Rauch et al., 2008, Attwell et al., 2010), the local neural activity and the spatial extent of the BOLD response are inconsistent.

We simulated the BOLD response in a spiking neural network. As explained in previous chapters, the BOLD mostly reflects the synaptic input than to output of neurons as it is more strongly linked to the local field potentials compared to spiking activity (Logothetis et al., 2001, Goense and Logothetis, 2008, Nir et al., 2008). Moreover, the well-known role of astrocytes and correspondingly glutamate in neurovascular coupling (Iadecola and Nedergaard, 2007, Koehler et al., 2009, Attwell et al., 2010, Petzold and Murthy, 2011) makes it plausible that the fMRI is more sensitive to the input of the neurons than their output.

In this study, we created a two-dimensional spiking network model of the visual cortex. Then, we compared the simulated network with both BOLD response and the estimated mean action potential outputs of the V1 neurons. Our model highlights the role of compartmental neurons to explain the observed spread of the BOLD response from the measurements.

2.3.1. Methods

The methods of this study include two parts: (i) fMRI experiment, and (ii) spiking neural network.

fMRI experiment

We conducted an fMRI experiment with sixteen subjects with normal or corrected-to-normal vision. Each session of the experiment contained 12 main and 3 multifocal localizer runs. The subjects were presented with wedge-shaped sinusoidal grating stimuli (Figure 2.5) presented at 43 cm distance on a back projection screen. The contrast and spatial frequency of the stimuli were 80% or 10%, and 0.5 or 2 cycles per degree, respectively. The data from the

two spatial frequencies were combined. The subjects fixated to a fixation cross at the center of the screen, and were engaged in an attention control task at the center of fixation (Larsson et al., 2006).

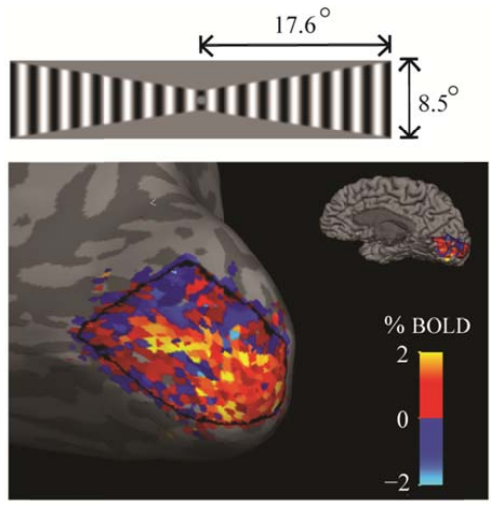

Figure 2.5. The wedge-shaped stimuli and representative individual BOLD signal change of a subject fixating to the center, superimposed to an inflated right hemisphere.

We used 3T MAGNETOM Skyra scanner (Siemens, Erlagen) with a 32-channel head coil. The 64x64x20 imaging data had 2.8 mm slice thickness and in-plane resolution (FOV = 180 mm) and were acquired with TR= 2.1 s and TE = 70 ms. Preprocessing included slice time correction, realignment, and reslicing However, we avoid spatial smoothing to keep high spatial resolution.

Two multifocal runs sampled the primary visual cortex. The positions of the localizer patches increased as a function of eccentricity and approximately followed human magnification factor (Schwartz, 1994, Duncan and Boynton, 2003). The cortical location of each data point of the individual subjects was thus mapped to the visual space. Then, these locations were in turn converted to the V1 model cortex coordinates, via the log-polar Schwartz transform (Schwartz, 1994, Duncan and Boynton, 2003).

Finally, we converted the BOLD signal into estimated cerebral blood flow signals (CBFe), following the balloon model (Buxton et al., 1998).

Spiking neural network

We created a two-dimensional network of exponential integrate-and-fire neurons to model of the visual cortex. We used Brian (Goodman and Brette, 2008) for the simulations. Primary visual cortex included both excitatory and inhibitory neurons which were evenly distributed on the model cortex with 0.23 mm distance between neurons. The number of V1 excitatory neurons in our model was 4 times higher than the inhibitory neurons. Figure 2.6 shows the connectivity of the neurons in different layers.

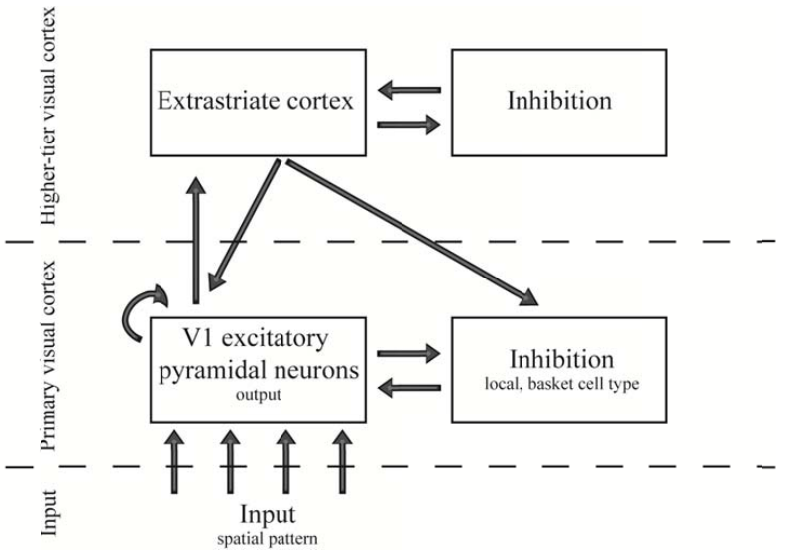

Figure 2.6. A schematic view of the spiking network layers and connections.

The pyramidal neurons of V1 comprised 6 compartments including: soma, a basal dendrite, and 4 serial compartments modeling the apical dendrite. The membrane voltage of the compartmental neurons in the soma was modeled with Equation 2.3.

$$C\frac{dV}{dt} = g_L(V_L - V) + \psi(V) + \sum I_{denrites}(t) \qquad (2.3)$$

$$\psi(V) = g_L \Delta_T \exp\left(\frac{V - V_T}{\Delta_T}\right)$$

where C is the membrane capacitance and g_L is the leak conductance. V_L determines the membrane potential at rest. $\psi(V)$ and V_T are the spiking current and the threshold, respectively. Δ_T, is the slope factor, which determines the voltage dependence of the spiking current. $I_{dendrites}$ represents ohmic currents flowing in from the dendritic compartments.

The input followed a Poisson distribution with a high firing probability at stimulus and lower probability (as a basal rate) elsewhere. For the rest of the connections between any neuron groups, the probability for the connections were stochastically generated and the total number of synapses decayed exponentially as a function of the cortical distance (Schwabe et al., 2006).

The model network was run for 500 ms, including 100 ms baseline to achieve a stable state, following 400ms stimulation. Then, the input activity of each V1

excitatory neuron was calculated as the mean glutamatergic conductance during stimulation, minus the baseline. The number of spikes was counted as the mean spike count during the stimulation. The time step for the simulation was 0.1 ms.

The simulation was validated by two measures: (i) we modeled the area summation function in V1 to estimate the spike output pattern to our stimulus (see section 2.4). In this way, we obtained predicted spiking responses of the V1 neurons to the stimulus. The spike response of excitatory neurons in V1 was compared to the estimated spiking output of V1 neurons. (ii) In the second measure, the excitatory synaptic conductance mediated by glutamate release in the presynaptic terminals of V1 excitatory neurons was compared to estimated blood flow signal from measured fMRI data. We used the Mean Squared Error (MSE) over the N samples in the 2mm x 2mm grid as:

$$MSE_{tot} = \sum_{i} (R_{spk,\mathrm{model},i} - R_{spk,\mathrm{target},i})^2 \Big/ N + \sum_{i} (R_{ge,\mathrm{model},i} - R_{CBF,\mathrm{target},i})^2 \Big/ N \tag{2.4}$$

where, for sample i, $R_{spk,model,i}$ is the normalized mean spike count, $R_{spk,target,i}$ is the area summation target (see section 2.4), $R_{ge,model,i}$ is the mean change in the excitatory conductance for the V1 excitatory neurons, and $R_{CBFe,target,}$ is the estimated cortical blood flow from the fMRI measurement. We used logarithm of the normalized original responses to reduce the noise contribution.

For the open parameters of the simulation, we chose parameter combinations with reasonably good output and dynamic range to have a better search of the parameter space. Then, we tried to search for the optimum value for two parameters: (i) number of connections to and from the extrastriate cortex and (ii) number of lateral connections on V1 to and from the inhibitory cells.

We run the simulation for two methods: (i) SOMA model: all inhibitory and excitatory synapses were connected to the soma of V1 excitatory neurons. However, the dendrites were still attached to the cell. (ii) DENDRITE model: the synapses were connected to the dendritic compartments. The feedforward and local connections were connected to the proximal dendritic compartments. The feedbacks were organized in one of the following structures: (i) distal: large distribution of feedback synapses to the distal compartments, (ii) middle: equal distribution to all apical compartments, or (iii) proximal: large distribution of synapses to the proximal compartments. In searching through the parameter space, we had 2 open parameters: number of connections to and from the extrastriate cortex and number of lateral connections on V1 to and from the inhibitory cells. In addition to these two open parameters, we searched through these feedback distributions as the third independent variable in our simulations.

2.3.2. Results

We quantified the spatial spread of the BOLD response in the primary visual cortex. To compare the spread in BOLD and spiking responses, we compared their normalized amplitudes outside the primary stimulus area. The relative amplitude of CBFe component was higher in the low contrast compared to high contrast stimuli. In parallel, the spike response was compared to the estimated activation pattern based on the area summation model. The difference between the two neural activation patterns was similar in the responses to high and low (Figure 2.7) contrast stimulus.

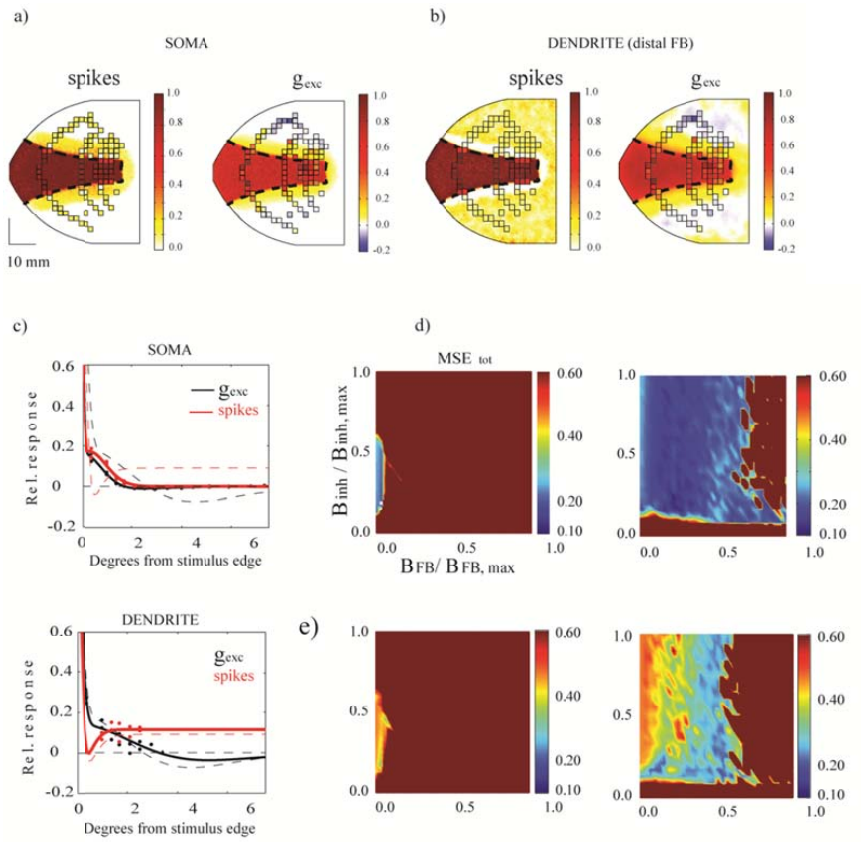

Figure 2.7. Distal feedback to V1 neurons bridges fMRI data to the neuronal spike rates. a) The best SOMA-model for the high contrast stimulus. The respective data samples (squares) are superimposed on the model simulation output (background colors). b) The best DENDRITE model with distal feedback. c) Comparison between model simulation output (continuous curves) and respective data (dashed curves). d) The error, MSE_{tot}, for the high contrast data, as a function of V1 inhibition (B_{inh}) and extrastriate feedback strength (B_{FB}) for the SOMA (left) and the DENDRITE model with distal feedback (right). e) As in d, for the low contrast stimulus.

Our simulations show (Figure 2.7) that the neural responses cannot be replicated with SOMA model. However, in case of DENDRITE model, the neural

response was best predicted by widely tuned feedback from the extrastriate cortex arriving to the distal dendrites for both high and the low contrast stimuli. Overall MSE_{tot} was 40% lower for DENDRITE, compared to SOMA model. The landscapes of the goodness measure (MSE_{tot}, Figure 2.7 d,e, showing the high and low-contrast data, respectively) show that the SOMA model is more unstable with changes of the parameters and has a narrower land of minimum MSE_{tot}, compared to DENDRITE model. The goodness of fit decreased sharply by changing the distribution of feedback synapses from distal towards proximal compartments and finally to the SOMA model.

2.4. Study IV: Contextual modulation of receptive field increases efficiency in modelled visual cortex

Contextual modulation is a well-known phenomenon (Maffei and Fiorentini, 1976, Knierim and van Essen, 1992, Levitt and Lund, 1997, Sceniak et al., 1999, Li et al., 2000, Felsen et al., 2005). In the primary visual cortex, area summation function (Sceniak et al., 1999, Angelucci et al., 2002, Cavanaugh et al., 2002) is an expression of contextual modulation at single-cell level. Earlier studies associated contextual modulation with efficient coding, such as increase of population sparseness and decorrelation of neural responses in the V1 (Vinje and Gallant, 2000). Therefore, in this study we wanted to see if there is a link between the ASF and coding efficiency in visually responsive neurons. We used the quantitative data from macaque cortex and a mathematical description of the ASF (Cavanaugh et al., 2002) together with a the biomimetic spiking neural network simulator of the primary visual cortex (see section 2.3) to quantitatively see the relation between the ASF and three coding efficiency metrics: (i) number of spikes, (ii) entropy per spike and (iii) population sparseness. We simulated the response of the primary visual cortex to natural stimuli and compared it to a predicted spike output in the visual cortex, calculated from the existing ASF data of primate V1 neurons (Cavanaugh et al., 2002), in relation to the three efficiency metrics.

2.4.1. Methods

For single neuron in a specific eccentricity, Cavanaugh et al. (2002) measured the (i) grating summation field, (ii) surround diameter and (iii) suppression levels in a typical ASF response curve (see section 1.4.2). In the estimation of the area summation target, we used a linear regression to the measured values in order to model each parameter as a function of eccentricity. In addition, we used mathematical modeling provided by Cavanaugh et al. (2002) for the neural response R(x):

$$R(x) = \frac{k_c L_c(x)}{1 + k_s L_s(x)}$$

$$L_c(x) = \left(\frac{2}{\sqrt{\pi}} \int_0^x e^{-(y/w_c)^2} dy \right)^2 \qquad (2.5)$$

$$L_s(x) = \left(\frac{2}{\sqrt{\pi}} \int_0^x e^{-(y/w_s)^2} dy \right)^2$$

where x is the diameter of circular stimulus, and L_c and L_s are the summed squared activations of the center and surround mechanisms, respectively. Furthermore, [k_c, k_s] and [w_c, w_s] are the gain and spatial extent coefficients for the center and surround components, respectively.

In our simulations to predict R(x) for each neuron in the primary visual cortex, we used the Nelder-Mead simplex optimization algorithm (Lagarias et al., 1998) to estimate k_c, k_s, w_c and w_s in Equation 2.5. We then used R(x) to figure out the expected neural responses for any input stimuli. In this study, specifically, we used 20 grayscale natural images from an image set provided by van Hateren and van der Schaaf (1998). For this purpose, we first convert the grayscale images to contrast stimuli to obtain the spatial structure of contrast energy by filtering the natural gray-scale images. In this filter, we used five different Gabor filter frequencies including 1, 2, 4, 8 and 16 cycles per 5° field of view, eight orientations, each with 0° and 90° offset phases (Kay et al., 2008).

Equation 2.5 gives the response for sum of all inputs. Therefore, if we assume a homogeneous distribution of the pixels in the visual field for a pixel at location (u,v) and distance r, the response function f(u,v) can be obtain from the derivative of R(x):

$$f(u,v) = R'(2r) \Big/ \pi r$$

$$r^2 = u^2 + v^2$$

$$R'(x) = \frac{k_c L'_c(x)(1 + k_s L_s(x)) - k_s L'_s(x) k_c L_c(x)}{(1 + k_s L_s(x))^2} \qquad (2.6)$$

$$L'_c(x) = \frac{8}{\pi} e^{-(xw_c)^2} \int e^{-(y/w_c)^2} dy$$

$$L'_s(x) = \frac{8}{\pi} e^{-(xw_s)^2} \int e^{-(y/w_s)^2} dy$$

For each location (u,v), the f(u,v) was calculated with respect to its distance from the receptive field center of the cell; and then, multiplied with the image contrast. Finally all the responses were summed over a 7° diameter area surrounding the receptive field center of each neuron. This process was repeated for each neuron to be able to obtain the target neural activation pattern of the primary visual cortex. These target patterns were then compared to the model

simulation outputs. We also created two artificial ASFs, to control how the amount of suppression and size of the summation field are related to the network efficiency. One of the artificial ASFs had larger grating summation field and no suppression, and the other one had a smaller summation field and stronger suppression compared to natural ASF.

We divided the input stimuli into two groups based on the distribution of their spatial frequencies to control how different properties of input stimuli might affect our results. The 20 gray-scale natural images where then assigned into two groups based on the frequency histograms using a k-means clustering approach. Each group contained ten gray-scale images, one with predominantly low spatial frequencies and the other group with mixed frequencies images.

The natural images were filtered through a retina model before using them as the input to our simulator. This retina model consisted of midget cells covering 0.5° to 27° eccentricities of the visual field. The density of the filter was comparable with the midget cell density in human retina (Dacey, 1993). In a control simulation we used a 1/5 lower density of midget cells.

We used the simulator described in Section 2.3. In our simulation, the simulation time was 500 ms with 200 ms baseline followed by 300 ms of stimulation. We repeated the simulation for 20 retina-filtered grayscale natural images. For each image, the numbers of local and feedback connections in the network were varied to produce outputs with variable levels of biological realism resulting in 625 different simulations, similar to section 2.3. The simulated response patterns were then compared to the corresponding area summation target pattern. In each response pattern, we used the absolute distance between the simulated and target responses. Then, we summed them across all neurons (Distance to Area Summation, DAS). We used energy consumption, entropy per spike, and population sparseness as the efficiency measures for the simulation output patterns.

We defined energy consumption based on dephosphorylation of adenosine triphosphate (ATP) molecules usage. Based on a previous study (Attwell and Laughlin, 2001, Howarth et al., 2012) the total number of spike counts is linearly related to energy consumption of the neuron (plus a baseline) and can be a good measure of energy consumption.

To calculate the entropy per spike, we calculated the probability distribution (q) of the spike outputs from a histogram with 256 bins:

$$ES = E \big/ N_s$$
$$E = -\sum q \log_2 q \qquad (2.7)$$

where E, ES and N_s are entropy, entropy per spike and total number of spikes,

respectively.

The third measure of efficiency, population sparseness, was calculated as

$$S_p = \left\{1 - \left[\frac{\left(\sum_{n=1}^{N}\left(y_n/N\right)\right)^2}{\sum_{n=1}^{N}\left(y_n\right)^2/N}\right]\right\} \Big/ \left[1 - \frac{1}{N}\right] \quad (2.8)$$

where y_n is the mean firing rate of neuron n in the set on N neurons and Sp is population sparseness (Vinje and Gallant, 2000). In this formula, 0 and 1 indicate lowest and highest sparseness value, respectively.

2.4.2. Results

For all images and simulation parameters, we plotted the efficiency metrics as a function of DAS (Figure 2.8). The spike count (as a measure of energy consumption) was positively linked (Pearson correlation coefficient = 0.88, $p < 0.01$) to DAS (Figure 2.8a). In addition, entropy per spike (as a measure of amount of information that can be coded into the spike train) was negatively linked (Pearson correlation coefficient = - 0.59, $p < 0.01$) to DAS (Figure 2.8b). Moreover, neural population sparseness was negatively linked (Pearson correlation coefficient = -0.56, $p < 0.01$) to DAS (Figure 2.8c). All these measures show that efficiency of the simulated response patterns is correlated with the ability of the network to predict the ASF, although the relation was nonlinear and varied between images. In addition, comparing two changing parameters in our simulations, our results show that the lateral connections between V1 excitatory and inhibitory cells have clearly stronger effect on ASF-association compared to extrastriate feedback connections.

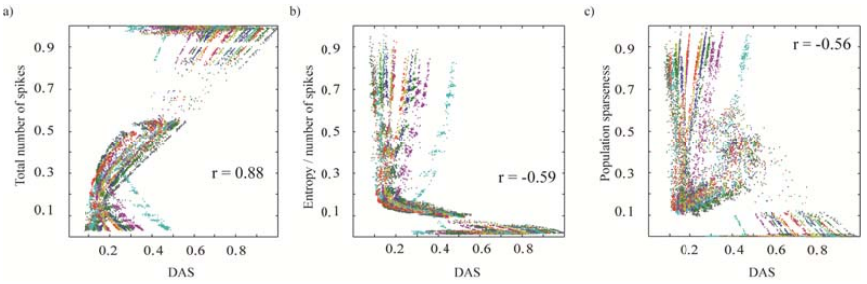

Figure 2.8. The efficiency of the spiking network, as a function of Distance to Area Summation (DAS). a) The relationship between the total number of spikes counted from V1 excitatory neurons (associated linearly with energy consumption) of simulated output patterns and similarity to estimated area summation target patterns. The data points in this plot represent the simulator output for the 20 images, each using 625 parameter combinations, with the data color coding for different images. 0.5° from the V1 model border, for all the patterns, were removed to avoid instability in borders. r corresponds to the correlation coefficient. b) The relationship

between entropy per spike of the simulated output patterns and DAS, with the same simulation output data and color coding as in panel a. c) The relationship between neural population sparseness (0 is minimum and 1 is maximum sparseness) of simulated output patterns and DAS, with the same simulation output data and color coding as panel a.

We divided the input stimuli into two sets, one including the images with stronger low frequencies and the other including the images with even distribution of spatial frequencies. The relationship between total number of spikes, entropy per spike, and population sparseness versus DAS show that the target ASF in our simulations is associated more strongly with efficient representation for the images containing primarily low frequency information. In our model, for simplicity we ignored the variability of receptive field parameters among neurons in similar eccentricities. The variability of the receptive field parameters might help capture a wider range of spatial frequencies in natural images and as a result reduce the variation in efficiency versus DAS between different stimuli.

In addition, in another analysis, we excluded the activation patterns which had very high or very low number of spikes (15% from top and bottom of the dynamic range of the total number of spikes) to avoid the parameter combinations that lead to unnatural saturated or low-responding activation patterns. By this exclusion, our results show a better association between the firing rate and entropy per spike versus DAS.

Then, we did two sets of control simulations. In the first, we decreased the resolution of the retina input to 1/5 of the original one. In this way, we had spatially larger filters, which probably cause a shift in the filter sensitivity towards lower spatial frequencies. The results show almost the same link between DAS and the efficiency measures compared to full-resolution retina. In the second set of control simulations, we replaced the compartmental neurons of excitatory V1 neurons with pointwise neurons. The results show that the compartmental neurons provide a better link between the efficiency of the network and DAS (Wilcoxon rank sum test with $p<0.05$).

Finally, with two artificial area summation functions, we tested if the natural ASF is optimized for the network efficiency. If so, we expect loss of efficiency by changing the form of ASF. Our results show that with the larger grating summation field and no suppression the entropy per spike is less relevant to the similarity to DAS compared to natural ASF. However, in case of having the smaller summation field and stronger suppression, the dependency between entropy per spike and DAS is similar to the natural ASF.

3. General discussion

In this thesis, I studied contextual modulation at macroscopic neural level and tried to find its link to efficiency of the neural network. Next, I participated in reviewing the challenges of predicting macroscopic neural responses based on single neurons. Then, I implemented a computational neural network and generalized response of single neurons to a population of neurons based on fMRI and theoretical contextual modulation data. Finally, employing this computational neural network, I was able to quantitatively establish the relationship between contextual modulation and efficiency of the neural network.

Contextual modulation associates with increased system-level neural network efficiency

In the first study of this thesis, we modulated the visual context around the center and measured the response with fMRI experiment. In summary, we show that cortical decorrelation model (Vanni and Rosenstrom, 2011) has the best explanatory power to predict interaction strength in our experimental data compared to other well-known contextual modulation models. In addition, we showed that in lower-order cortical areas, BOLD signal changes spread much further than what has been expected based on average receptive field size of the neurons in these areas. Moreover, our results suggest similar interaction mechanisms in all visual cortical areas. Finally, our results showed less suppression in lower-order cortical areas compared to higher-order areas.

Previous studies provide models of contextual modulation which are mainly based on divisive gain control mechanism (Foley, 1994, Sceniak et al., 2001, Xing and Heeger, 2001). However, we experimentally showed that in all studied cortical visual areas contextual modulation in macroscopic level is related to decorrelation of the cortical activation (Vanni and Rosenstrom, 2011) and subsequently, most likely is related to redundancy reduction in fMRI activation patterns. Therefore, as the main finding of this study, we claim that contextual modulation associates with increased system-level neural network efficiency. This is in line with previous contextual modulation studies (Vinje and Gallant, 2002, Felsen et al., 2005) which report a link between contextual modulation and decreases of redundancy in neural responses (Vinje and Gallant, 2002, Felsen et al., 2005).

The results showed that the contextual effect is present over very long distances in the visual field. This results in wide–spread BOLD signals; comparable

distant modulation has been also reported in earlier studies (Ichida et al., 2007, Nurminen et al., 2010). However, this spread of the BOLD signal cannot be directly explained by the length of horizontal connections in V1 reported in earlier anatomical and physiological study (Angelucci et al., 2002). This BOLD signal spread might be explained by rapidly conducting feedforward-feedback loops between the primary visual cortex and extra-striate areas (Bullier, 2001, Schwabe et al., 2006, Schwabe et al., 2010).

The results also confirms previous findings (Kastner et al., 2001, Zenger-Landolt and Heeger, 2003) that report less suppression in lower-order cortical areas compared to higher-order areas. Larger receptive fields of neurons in higher-order cortical areas might be the reason for this finding as it causes more average activation in the neighborhood of a cortical neuron.

Macroscopic cortical activation could be predicted by a computational neural network

In the second study of the present thesis, we reviewed possibilities, challenges and critical requirements to be able to model and ideally predict fMRI data. Such a modeling possibility comes through existing knowledge about the mechanisms of fMRI signal generation together with theoretical and experimental information about the single neuron processing. The ability of fMRI signal prediction would provide a significant contribution to better understanding of the visual system, with numerous applications in theoretical, experimental and clinical studies and even industry.

In short, we prepared a blueprint to predict experimental BOLD signal using a mesoscopic neural network simulator. Thus, this review confirms the feasibility of macroscopic cortical activation prediction by a computational neural network. Such a mesoscopic model avoids the details of realistic neural network and provides systems-level simulations of neurons. This system-level simulation of neuronal population provides a very strong explanatory power to understand the principles of biological data processing in a hierarchical network.

However, such a mesoscopic neural network simulation faces many challenges due to incomplete current knowledge of the visual system and existing technical and computational limitations. Among the challenges, an indirect relationship between neural activity and fMRI signal is the most important source of confusion. Based on existing literature (for review see Section 2.2.2) the fMRI signal prediction should likely be based on excitatory synaptic input (glutamate release). As a consequence, to be able to access tuning properties of excitatory synaptic input rather than spiking output, it is necessary to include compartmental neurons in mesoscopic neural network simulation for predicting fMRI data.

Dendrites have a key role in prediction of the contextual modulation and macroscopic cortical responses

In the third study of this thesis, we designed a simulation of the visual cortex, to predict the fMRI signal. This simulation was based on anatomical and biophysical information about realistic neural networks. One of the main goals of this fMRI signal prediction was to explain the spread of the BOLD response which could not yet be addressed by narrowly tuned action potentials. The BOLD response is better linked to the input of the neurons than the output (Iadecola and Nedergaard, 2007, Koehler et al., 2009, Attwell et al., 2010, Petzold and Murthy, 2011). Therefore, we hypothesized that the fundamental differences in BOLD and electrophysiology data might emerge from signal transformations between the input and the output of excitatory cortical neurons. Better fitting of post synaptic potentials rather than spike counts in our simulation results to corresponding experimental BOLD signal, provided a direct support for this hypothesis. I would like to note that using spin-echo fMRI experiment for this purpose was very important as it provided a good spatial resolution compared to gradient-echo fMRI sequences.

In addition, the control simulations with feedback only to soma confirm the crucial role of dendrites with feedback concentrated in the distal dendritic compartments to be able to predict the BOLD signal. This helped to achieve a better fit between the data and the model. Therefore, we claim that the point-like model of the neurons might significantly limit cerebral cortex modelling as they do not have a separate tuning function for input and output of the neurons.

In summary, we suggest that dendrites have a key role in prediction of the contextual modulation and macroscopic cortical responses.

Computational neural network suggest a strong link between contextual modulation and efficiency of the visual system

In the last study, we aimed to find the relationship between the area summation function and the efficiency of neural population code using a similar simulator of the visual cortex as in the third study. We showed that the area summation function (contextual modulation) is closely linked to efficiency of a network (specifically, energy consumption, information capacity, and population sparseness). This is in line with previous studies which link contextual modulation to sparse code representation of the visual input (Vinje and Gallant, 2000) or reduction of dependencies between single cells (Schwartz and Simoncelli, 2001).

In line with my third study, the results emphasized the role of dendritic compartment (Williams and Stuart, 2002) of excitatory V1 neurons to have a stronger association between area summation and the efficiency of the neural network. Moreover, interestingly we found a clear link between horizontal inhibitory connectivity and efficiency. This finding is in line with recent litera-

ture by Nurminen and Angelucci (2014) which claimed that horizontal connections have a specific role in network efficiency.

As a limitation, in our simulation results the link between efficiency measures and area summation was stronger for low-spatial frequencies input stimuli than mixed-frequencies stimuli. This might be due to having smaller number of cells in this model than a real visual cortex. Another reason might be the fact that in estimation of the area summation target, we averaged measured area summation function parameters in each eccentricity and the variability of the area summation parameters across neural data may help capture a wider range of spatial frequencies present in input stimuli. Moreover, our model is a simplification of the primate visual system and for example, our neurons only have spatial position but no orientation tuning, while orientation tuning might be a necessary feature to maximize the efficiency for image statistics in cortical representation of spatially neighboring edges (Geisler et al., 2001).

Future Prospects

Computational neural network models of the visual cortex provide fairly powerful means to analyze the visual system functions, without going to the complexity of very detailed simulation (Markram, 2006). However, this stimulation can be improved in several ways in future studies. Specifically, (i) to avoid the complexity of the network, we used reduced number of units in the neural network model, compared to the primate visual cortex. For example, we used one neuron representing 10^4 neuros in the cortex; this simplification might result in underestimation of local connections (although we tried to control it with stronger neural auto-feedback) roles and emphasizing the role of long distance connections in fMRI responses. Beside a closer number of neurons to biological reality, including biological diversity in the inhibitory neurons with different roles in cortical information processing would bring a considerable improvement in computing power. (ii) In the simulations, we only used one higher cortical visual area and ignored corticothalamic feedback. This would result in refusing many useful higher-order source of information such as attention, adaptation and learning. (iii) We ignored the layered structure of the primate cerebral cortex and modeled all neural activation with one layer. However, each cortical layer has a preferable set of neuron types and neural connectivity (Nieuwenhuys, 1994, Douglas and Martin, 2004) and thus might contribute to different data processing roles (Grossberg, 2007). (iv) The neural network model has no orientation, speed, disparity, spatial frequency, ocular dominance or wavelength tuning of the neurons, which might result in missing affective neural features in efficient neural coding.

In general, a more realistic model would help us to have a better understanding of how the visual system processes information at different level of details. Such a model would also have many clinical applications as it might help us to figure out the origins of the visual system disorders by providing better understanding of brain functions associated with normal and abnormal vision.

4. Conclusion

In conclusion, in this PhD study, I investigated system-level contextual modulation in human visual system. I used both experimental and theoretical approaches to find the mechanism underlying contextual modulation. The results of this study highlight the role of contextual modulation to achieve efficiency in a neural network. In addition, the results of the present study suggest that contextual modulation affects the information transmission efficiency; this change is observable even in macroscopic population response of neurons. In addition, using only point-like model of the neurons in cortical simulations might be a significant limitation.

References

Aguirre GK, Zarahn E, D'Esposito M (1998) The variability of human, BOLD hemodynamic responses. Neuroimage 8:360-369.

Alitto HJ, Usrey WM (2003) Corticothalamic feedback and sensory processing. Current opinion in neurobiology 13:440-445.

Andersson JL, Hutton C, Ashburner J, Turner R, Friston K (2001) Modeling geometric deformations in EPI time series. Neuroimage 13:903-919.

Angelucci A, Levitt JB, Walton EJ, Hupe JM, Bullier J, Lund JS (2002) Circuits for local and global signal integration in primary visual cortex. Journal of Neuroscience 22:8633-8646.

Arbib MA (ed.) (2003) The Handbook of Brain Theory and Neural Networks. London: MIT Press.

Attwell D, Buchan AM, Charpak S, Lauritzen M, Macvicar BA, Newman EA (2010) Glial and neuronal control of brain blood flow. Nature 468:232-243.

Attwell D, Laughlin SB (2001) An energy budget for signaling in the grey matter of the brain. Journal of cerebral blood flow and metabolism : official journal of the International Society of Cerebral Blood Flow and Metabolism 21:1133-1145.

Averbeck BB, Latham PE, Pouget A (2006) Neural correlations, population coding and computation. Nature reviews Neuroscience 7:358-366.

Barlow H (1961) Possible principles underlying the transformation of sensory messages, Sensory Communication: W. Rosenblith. Cambridge, MA, MIT Press: 217-234.

Barlow H, Földiak P (1989) Adaptation and decorrelation in the cortex. In: The Computing Neuron(Richard, D. et al., eds), pp 54-72 Boston: Addison-Wesley Longman Publishing Co.

Barone P, Batardiere A, Knoblauch K, Kennedy H (2000) Laminar distribution of neurons in extrastriate areas projecting to visual areas V1 and V4 correlates with the hierarchical rank and indicates the operation of a distance rule. The Journal of neuroscience : the official journal of the Society for Neuroscience 20:3263-3281.

Bernander O, Koch C, Douglas RJ (1994) Amplification and linearization of distal synaptic input to cortical pyramidal cells. J Neurophysiol 72:2743-2753.

Boorman L, Kennerley AJ, Johnston D, Jones M, Zheng Y, Redgrave P, Berwick J (2010) Negative blood oxygen level dependence in the rat: a model for investigating the role of suppression in neurovascular coupling. J Neurosci 30:4285-4294.

Boynton GM, Hegde J (2004) Visual cortex: the continuing puzzle of area V2. Current biology : CB 14:R523-524.

Branco T, Hausser M (2010) The single dendritic branch as a fundamental functional unit in the nervous system. Curr Opin Neurobiol 20:494-502.

Brenner N, Bialek W, de Ruyter van Steveninck R (2000) Adaptive rescaling maximizes information transmission. Neuron 26:695-702.

Brunel N, van Rossum MCW (2007) Lapicque's 1907 paper: from frogs to integrate-and-fire. Biological Cybernetics 97:337-339.

Bullier J (2001) Integrated model of visual processing. Brain Research 36:96-107.

Burkitt AN (2006a) A review of the integrate-and-fire neuron model: I. Homogeneous synaptic input. Biol Cybern 95:1-19.

Burkitt AN (2006b) A review of the integrate-and-fire neuron model: II. Inhomogeneous synaptic input and network properties. Biological cybernetics 95:97-112.

Burns ME, Lamb TD (2004) Visual Transduction by Rod and Cone Photoreceptors. In: Visual Neuroscience: Massachusetts Institute of Technology.

Buxton RB, Wong EC, Frank LR (1998) Dynamics of blood flow and oxygenation changes during brain activation: the balloon model. Magnetic resonance in medicine : official journal of the Society of Magnetic Resonance in Medicine / Society of Magnetic Resonance in Medicine 39:855-864.

Calamante F, Thomas DL, Pell GS, Wiersma J, Turner R (1999) Measuring cerebral blood flow using magnetic resonance imaging techniques. J Cereb Blood Flow Metab 19:701-735.

Callaway EM (2005) Structure and function of parallel pathways in the primate early visual system. J Physiol 566:13-19.

Campbell FW, Cooper GF, Enroth-Cugell C (1969) The spatial selectivity of the visual cells of the cat. J Physiol 203:223-235.

Campbell FW, Kulikowski JJ, Levinson J (1966) The effect of orientation on the visual resolution of gratings. J Physiol 187:427-436.

Cannon MW, Fullenkamp SC (1991) Spatial Interactions in Apparent Contrast - Inhibitory Effects among Grating Patterns of Different Spatial-Frequencies, Spatial Positions and Orientations. Vision Research 31.

Cannon MW, Fullenkamp SC (1993) Spatial interactions in apparent contrast: individual differences in enhancement and suppression effects. Vision Research 33:1685-1695.

Cavanaugh JR, Bair W, Movshon JA (2002) Nature and interaction of signals from the receptive field center and surround in macaque V1 neurons. Journal of Neurophysiology 88:2530-2546.

Chubb C, Sperling G, Solomon JA (1989) Texture interactions determine perceived contrast. Proc Natl Acad Sci U S A 86:9631-9635.

Dacey DM (1993) The mosaic of midget ganglion cells in the human retina. J Neurosci 13:5334-5355.

Deco G, Jirsa VK, Robinson PA, Breakspear M, Friston K (2008) The dynamic brain: from spiking neurons to neural masses and cortical fields. PLoS Comput Biol 4:e1000092.

Devor A, Tian P, Nishimura N, Teng IC, Hillman EM, Narayanan SN, Ulbert I, Boas DA, Kleinfeld D, Dale AM (2007) Suppressed neuronal activity and concurrent arteriolar vasoconstriction may explain negative blood oxygenation level-dependent signal. J Neurosci 27:4452-4459.

Devor A, Ulbert I, Dunn AK, Narayanan SN, Jones SR, Andermann ML, Boas DA, Dale AM (2005) Coupling of the cortical hemodynamic response to cortical and thalamic neuronal activity. Proc Natl Acad Sci U S A 102:3822-3827.

Douglas RJ, Martin KA (2004) Neuronal circuits of the neocortex. Annu Rev Neurosci 27:419-451.

Dumoulin SO, Hess RF (2006) Modulation of V1 activity by shape: image-statistics or shape-based perception? J Neurophysiol 95:3654-3664.

Duncan RO, Boynton GM (2003) Cortical magnification within human primary visual cortex correlates with acuity thresholds. Neuron 38:659-671.

Euler T, Haverkamp S, Schubert T, Baden T (2014) Retinal bipolar cells: elementary building blocks of vision. Nat Rev Neurosci 15:507-519.

Fairhall AL, Lewen GD, Bialek W, de Ruyter Van Steveninck RR (2001) Efficiency and ambiguity in an adaptive neural code. Nature 412:787-792.

Felleman DJ, Van Essen DC (1991a) Distributed hierarchical processing in the primate cerebral cortex. Cereb Cortex 1:1-47.
Felleman DJ, Van Essen DC (1991b) Distributed hierarchical processing in the primate cerebral cortex. Cerebral Cortex 1:1-47.
Felsen G, Touryan J, Dan Y (2005) Contextual modulation of orientation tuning contributes to efficient processing of natural stimuli. Network 16:139-149.
Field DJ (1987) Relations between the statistics of natural images and the response properties of cortical cells. J Opt Soc Am A 4:2379-2394.
Field GD, Chichilnisky EJ (2007) Information processing in the primate retina: circuitry and coding. Annual review of neuroscience 30:1-30.
Foley JM (1994) Human Luminance Pattern-Vision Mechanisms - Masking Experiments Require a New Model. J Opt Soc Am A 11:1710-1719.
Fourcaud-Trocme N, Hansel D, van Vreeswijk C, Brunel N (2003) How spike generation mechanisms determine the neuronal response to fluctuating inputs. J Neurosci 23:11628-11640.
Friston K (2010) The free-energy principle: a unified brain theory? Nat Rev Neurosci 11:127-138.
Friston KJ, Ashburner JT, Kiebel S, Nichols TE, Penny WD (eds.) (2007) Statistical Parametric Mapping: The Analysis of Functional Brain Images: Academic Press.
Friston KJ, Williams S, Howard R, Frackowiak RS, Turner R (1996) Movement-related effects in fMRI time-series. Magn Reson Med 35:346-355.
Geisler WS, Perry JS, Super BJ, Gallogly DP (2001) Edge co-occurrence in natural images predicts contour grouping performance. Vision Res 41:711-724.
Gilbert CD, Wiesel TN (1990) The influence of contextual stimuli on the orientation selectivity of cells in primary visual cortex of the cat. Vision Res 30:1689-1701.
Goense J, Merkle H, Logothetis NK (2012) High-resolution fMRI reveals laminar differences in neurovascular coupling between positive and negative BOLD responses. Neuron 76:629-639.
Goense JB, Logothetis NK (2006) Laminar specificity in monkey V1 using high-resolution SE-fMRI. Magn Reson Imaging 24:381-392.
Goense JB, Logothetis NK (2008) Neurophysiology of the BOLD fMRI signal in awake monkeys. Current biology : CB 18:631-640.
Gollo LL, Kinouchi O, Copelli M (2009) Active dendrites enhance neuronal dynamic range. PLoS Comput Biol 5:e1000402.
Goodman D, Brette R (2008) Brian: a simulator for spiking neural networks in python. Frontiers in neuroinformatics 2:5.
Grill-Spector K, Kushnir T, Edelman S, Avidan G, Itzchak Y, Malach R (1999) Differential processing of objects under various viewing conditions in the human lateral occipital complex. Neuron 24:187-203.
Grill-Spector K, Malach R (2001) fMR-adaptation: a tool for studying the functional properties of human cortical neurons. Acta psychologica 107:293-321.
Grill-Spector K, Malach R (2004) The human visual cortex. Annual review of neuroscience 27:649-677.
Grossberg S (2007) Towards a unified theory of neocortex: laminar cortical circuits for vision and cognition. Prog Brain Res 165:79-104.
Gulyas B, Orban GA, Duysens J, Maes H (1987) The suppressive influence of moving textured backgrounds on responses of cat striate neurons to moving bars. Journal of Neurophysiology 57:1767-1791.
Haxby JV, Gobbini MI, Furey ML, Ishai A, Schouten JL, Pietrini P (2001) Distributed and overlapping representations of faces and objects in ventral temporal cortex. Science 293:2425-2430.

Haydon PG, Carmignoto G (2006) Astrocyte control of synaptic transmission and neurovascular coupling. Physiological reviews 86:1009-1031.

Henriksson L, Karvonen J, Salminen-Vaparanta N, Railo H, Vanni S (2012) Retinotopic maps, spatial tuning, and locations of human visual areas in surface coordinates characterized with multifocal and blocked FMRI designs. Plos One 7:e36859.

Hodgkin AL, Huxley AF (1952) A quantitative description of membrane current and its application to conduction and excitation in nerve. J Physiol 117:500-544.

Howarth C, Gleeson P, Attwell D (2012) Updated energy budgets for neural computation in the neocortex and cerebellum. Journal of cerebral blood flow and metabolism : official journal of the International Society of Cerebral Blood Flow and Metabolism 32:1222-1232.

Hu X, Yacoub E (2012) The story of the initial dip in fMRI. Neuroimage 62:1103-1108.

Hubel DH, Wiesel TN (1959) Receptive fields of single neurones in the cat's striate cortex. J Physiol 148:574-591.

Hubel DH, Wiesel TN (1962) Receptive fields, binocular interaction and functional architecture in the cat's visual cortex. J Physiol 160:106-154.

Hubel DH, Wiesel TN (1968) Receptive fields and functional architecture of monkey striate cortex. J Physiol 195:215-243.

Huettel SA, Song AW, McCarthy G (2004) Functional Magnetic Resonance Imaging: Sinauer Associates.

Hyvärinen A, Hurri J, Hoyer PO (2009) Natural Image Statistics— A probabilistic approach to early computational vision: Springer-Verlag.

Iadecola C, Nedergaard M (2007) Glial regulation of the cerebral microvasculature. Nature neuroscience 10:1369-1376.

Ichida JM, Schwabe L, Bressloff PC, Angelucci A (2007) Response facilitation from the "suppressive" receptive field surround of macaque V1 neurons. Journal of Neurophysiology 98:2168-2181.

Jia H, Rochefort NL, Chen X, Konnerth A (2010) Dendritic organization of sensory input to cortical neurons in vivo. Nature 464:1307-1312.

Kaplan E (2004) The M, P, and K Pathways of the Primate Visual System. In: Visual Neuroscience: Massachusetts Institute of Technology.

Kastner S, De Weerd P, Pinsk MA, Elizondo MI, Desimone R, Ungerleider LG (2001) Modulation of sensory suppression: Implications for receptive field sizes in the human visual cortex. Journal of Neurophysiology 86:1398-1411.

Kay KN, Naselaris T, Prenger RJ, Gallant JL (2008) Identifying natural images from human brain activity. Nature 452:352-355.

Knierim JJ, van Essen DC (1992) Neuronal responses to static texture patterns in area V1 of the alert macaque monkey. Journal of Neurophysiology 67:961-980.

Koehler RC, Roman RJ, Harder DR (2009) Astrocytes and the regulation of cerebral blood flow. Trends Neurosci 32:160-169.

Koopmans PJ, Barth M, Norris DG (2010) Layer-specific BOLD activation in human V1. Hum Brain Mapp 31:1297-1304.

Kuffler SW (1953) Discharge patterns and functional organization of mammalian retina. J Neurophysiol 16:37-68.

Lagarias JC, Reeds JA, Wright MH, Wright PE (1998) Convergence Properties of the Nelder-Mead Simplex Method in Low Dimensions. SIAM J OPTIM 9:112-147.

Larsson J, Landy MS, Heeger DJ (2006) Orientation-selective adaptation to first- and second-order patterns in human visual cortex. Journal of neurophysiology 95:862-881.

Laughlin S (1981) A simple coding procedure enhances a neuron's information capacity. Z Naturforsch C 36:910-912.
Lennie P, Movshon JA (2005) Coding of color and form in the geniculostriate visual pathway (invited review). Journal of the Optical Society of America A, Optics, image science, and vision 22:2013-2033.
Leuba G, Kraftsik R (1994) Changes in volume, surface estimate, three-dimensional shape and total number of neurons of the human primary visual cortex from midgestation until old age. Anatomy and embryology 190:351-366.
Levitt JB, Lund JS (1997) Contrast dependence of contextual effects in primate visual cortex. Nature 387:73-76.
Levitt JB, Lund JS (2002) The spatial extent over which neurons in macaque striate cortex pool visual signals. Visual Neuroscience 19:439-452.
Li W, Thier P, Wehrhahn C (2000) Contextual influence on orientation discrimination of humans and responses of neurons in V1 of alert monkeys. Journal of Neurophysiology 83:941-954.
Lin AL, Fox PT, Hardies J, Duong TQ, Gao JH (2010) Nonlinear coupling between cerebral blood flow, oxygen consumption, and ATP production in human visual cortex. Proc Natl Acad Sci U S A 107:8446-8451.
Livingstone M, Hubel D (1988) Segregation of form, color, movement, and depth: anatomy, physiology, and perception. Science 240:740-749.
Logothetis NK (2008) What we can do and what we cannot do with fMRI. Nature 453:869-878.
Logothetis NK, Pauls J, Augath M, Trinath T, Oeltermann A (2001) Neurophysiological investigation of the basis of the fMRI signal. Nature 412:150-157.
Maffei L, Fiorentini A (1976) The unresponsive regions of visual cortical receptive fields. Vision Research 16:1131-1139.
Magri C, Logothetis NK, Panzeri S (2011) Investigating static nonlinearities in neurovascular coupling. Magnetic resonance imaging 29:1358-1364.
Markov NT, Misery P, Falchier A, Lamy C, Vezoli J, Quilodran R, Gariel MA, Giroud P, Ercsey-Ravasz M, Pilaz LJ, Huissoud C, Barone P, Dehay C, Toroczkai Z, Van Essen DC, Kennedy H, Knoblauch K (2011) Weight consistency specifies regularities of macaque cortical networks. Cereb Cortex 21:1254-1272.
Markram H (2006) The blue brain project. Nat Rev Neurosci 7:153-160.
Martin R, Grünert U (2004) Ganglion Cells in Mammalian Retinae. In: Visual neuroscience: Massachusetts Institute of Technology.
McAlonan K, Cavanaugh J, Wurtz RH (2008) Guarding the gateway to cortex with attention in visual thalamus. Nature 456:391-394.
McDonald JS, Seymour KJ, Schira MM, Spehar B, Clifford CWG (2009) Orientation-specific contextual modulation of the fMRI BOLD response to luminance and chromatic gratings in human visual cortex. Vision Research 49:1397-1405.
Megias M, Emri Z, Freund TF, Gulyas AI (2001) Total number and distribution of inhibitory and excitatory synapses on hippocampal CA1 pyramidal cells. Neuroscience 102:527-540.
Mitchell TM, Shinkareva SV, Carlson A, Chang KM, Malave VL, Mason RA, Just MA (2008) Predicting human brain activity associated with the meanings of nouns. Science 320:1191-1195.
Mountcastle VB (1997) The columnar organization of the neocortex. Brain 120 (Pt 4):701-722.
Muller JR, Metha AB, Krauskopf J, Lennie P (1999) Rapid adaptation in visual cortex to the structure of images. Science 285:1405-1408.

Naud R, Marcille N, Clopath C, Gerstner W (2008) Firing patterns in the adaptive exponential integrate-and-fire model. Biological cybernetics 99:335-347.
Nelson R, Kolb H (2004) ON and OFF Pathways in the Vertebrate Retina and Visual System. In: Visual neuroscience: Massachusetts Institute of Technology.
Nieuwenhuys R (1994) The neocortex. An overview of its evolutionary development, structural organization and synaptology. Anatomy and embryology 190:307-337.
Nir Y, Dinstein I, Malach R, Heeger DJ (2008) BOLD and spiking activity. Nature neuroscience 11:523-524; author reply 524.
Nir Y, Fisch L, Mukamel R, Gelbard-Sagiv H, Arieli A, Fried I, Malach R (2007) Coupling between neuronal firing rate, gamma LFP, and BOLD fMRI is related to interneuronal correlations. Curr Biol 17:1275-1285.
Nurminen L, Angelucci A (2014) Multiple components of surround modulation in primary visual cortex: Multiple neural circuits with multiple functions? Vision Research.
Nurminen L, Peromaa T, Laurinen P (2010) Surround suppression and facilitation in the fovea: very long-range spatial interactions in contrast perception. Journal of Vision.
Ogawa S, Lee TM, Kay AR, Tank DW (1990) Brain magnetic resonance imaging with contrast dependent on blood oxygenation. Proc Natl Acad Sci U S A 87:9868-9872.
Olshausen BA, Field DJ (1996) Emergence of simple-cell receptive field properties by learning a sparse code for natural images. Nature 381:607-609.
Olzak LA, Laurinen PI (1999) Multiple gain control processes in contrast-contrast phenomena. Vision Res 39:3983-3987.
Orban GA (2008) Higher order visual processing in macaque extrastriate cortex. Physiological reviews 88:59-89.
Ozeki H, Finn IM, Schaffer ES, Miller KD, Ferster D (2009) Inhibitory stabilization of the cortical network underlies visual surround suppression. Neuron 62:578-592.
Pasley BN, Inglis BA, Freeman RD (2007) Analysis of oxygen metabolism implies a neural origin for the negative BOLD response in human visual cortex. Neuroimage 36:269-276.
Petzold GC, Murthy VN (2011) Role of astrocytes in neurovascular coupling. Neuron 71:782-797.
Pihlaja M, Henriksson L, James AC, Vanni S (2008) Quantitative multifocal fMRI shows active suppression in human V1. Human Brain Mapping 29:1001-1014.
Pinotsis DA, Friston KJ (2011) Neural fields, spectral responses and lateral connections. Neuroimage 55:39-48.
Pinotsis DA, Moran RJ, Friston KJ (2012) Dynamic causal modeling with neural fields. Neuroimage 59:1261-1274.
Poirazi P, Brannon T, Mel BW (2003) Pyramidal neuron as two-layer neural network. Neuron 37:989-999.
Polimeni JR, Fischl B, Greve DN, Wald LL (2010) Laminar analysis of 7T BOLD using an imposed spatial activation pattern in human V1. Neuroimage 52:1334-1346.
Polsky A, Mel BW, Schiller J (2004) Computational subunits in thin dendrites of pyramidal cells. Nat Neurosci 7:621-627.
Raichle ME, Mintun MA (2006) Brain work and brain imaging. Annual review of neuroscience 29:449-476.
Rakic P (2008) Confusing cortical columns. Proc Natl Acad Sci U S A 105:12099-12100.

Rao RP, Ballard DH (1999) Predictive coding in the visual cortex: a functional interpretation of some extra-classical receptive-field effects. Nat Neurosci 2:79-87.
Rauch A, Rainer G, Logothetis NK (2008) The effect of a serotonin-induced dissociation between spiking and perisynaptic activity on BOLD functional MRI. Proceedings of the National Academy of Sciences of the United States of America 105:6759-6764.
Reich DS, Mechler F, Victor JD (2001) Temporal coding of contrast in primary visual cortex: when, what, and why. J Neurophysiol 85:1039-1050.
Reina-De La Torre F, Rodriguez-Baeza A, Sahuquillo-Barris J (1998) Morphological characteristics and distribution pattern of the arterial vessels in human cerebral cortex: a scanning electron microscope study. Anat Rec 251:87-96.
Ress D, Glover GH, Liu J, Wandell B (2007) Laminar profiles of functional activity in the human brain. Neuroimage 34:74-84.
Ringach DL (2004) Mapping receptive fields in primary visual cortex. J Physiol 558:717-728.
Rivadulla C, Sharma J, Sur M (2001) Specific roles of NMDA and AMPA receptors in direction-selective and spatial phase-selective responses in visual cortex. J Neurosci 21:1710-1719.
Saalmann YB, Kastner S (2009) Gain control in the visual thalamus during perception and cognition. Current opinion in neurobiology 19:408-414.
Sceniak MP, Hawken MJ, Shapley R (2001) Visual spatial characterization of macaque V1 neurons. Journal of Neurophysiology 85:1873-1887.
Sceniak MP, Ringach DL, Hawken MJ, Shapley R (1999) Contrast's effect on spatial summation by macaque V1 neurons. Nat Neurosci 2:733-739.
Schwabe L, Ichida JM, Shushruth S, Mangapathy P, Angelucci A (2010) Contrast-dependence of surround suppression in Macaque V1: Experimental testing of a recurrent network model. Neuroimage.
Schwabe L, Obermayer K, Angelucci A, Bressloff PC (2006) The role of feedback in shaping the extra-classical receptive field of cortical neurons: A recurrent network model. Journal of Neuroscience 26:9117-9129.
Schwartz EL (1994) Computational Studies of the Spatial Architecture of Primate Visual Cortex: Columns, Maps and Protomaps. . In: Cerebral Cortex: Volume 10: Primary Visual Cortex in Primates(Peters, A. and Rockland, K. S., eds), pp 359-442 New York and London: Plenum Press.
Schwartz O, Simoncelli EP (2001) Natural signal statistics and sensory gain control. Nat Neurosci 4:819-825.
Sejnowski TJ, Koch C, Churchland PS (1988) Computational neuroscience. Science 241:1299-1306.
Shannon CE (1948) A Mathematical theory of communication. The Bell System Technical Journal 27:379-423.
Sharifian F, Nurminen L, Vanni S (2013) Visual interactions conform to pattern decorrelation in multiple cortical areas. Plos One 8:e68046.
Sharpee TO, Sugihara H, Kurgansky AV, Rebrik SP, Stryker MP, Miller KD (2006) Adaptive filtering enhances information transmission in visual cortex. Nature 439:936-942.
Shmuel A, Augath M, Oeltermann A, Logothetis NK (2006) Negative functional MRI response correlates with decreases in neuronal activity in monkey visual area V1. Nat Neurosci 9:569-577.
Sidiropoulou K, Pissadaki EK, Poirazi P (2006) Inside the brain of a neuron. EMBO Rep 7:886-892.

Simoncelli EP, Olshausen BA (2001) Natural image statistics and neural representation. Annu Rev Neurosci 24:1193-1216.
Sjöstrom PJ, Rancz EA, Roth A, Hausser M (2008) Dendritic excitability and synaptic plasticity. Physiol Rev 88:769-840.
Snowden RJ, Hammett ST (1998) The effects of surround contrast on contrast thresholds, perceived contrast and contrast discrimination. Vision Res 38:1935-1945.
Solomon SG, Lee BB, Sun H (2006) Suppressive surrounds and contrast gain in magnocellular-pathway retinal ganglion cells of macaque. J Neurosci 26:8715-8726.
Somers DC, Todorov EV, Siapas AG, Toth LJ, Kim DS, Sur M (1998) A local circuit approach to understanding integration of long-range inputs in primary visual cortex. Cereb Cortex 8:204-217.
Spruston N (2008) Pyramidal neurons: dendritic structure and synaptic integration. Nat Rev Neurosci 9:206-221.
Spruston N, Jaffe DB, Johnston D (1994) Dendritic attenuation of synaptic potentials and currents: the role of passive membrane properties. Trends Neurosci 17:161-166.
Tajima S, Watanabe M, Imai C, Ueno K, Asamizuya T, Sun P, Tanaka K, Cheng K (2010) Opposing effects of contextual surround in human early visual cortex revealed by functional magnetic resonance imaging with continuously modulated visual stimuli. Journal of Neuroscience, DOI 30:3264-3270.
Tsodyks MV, Skaggs WE, Sejnowski TJ, McNaughton BL (1997) Paradoxical effects of external modulation of inhibitory interneurons. Journal of Neuroscience 17:4382-4388.
Ungerleider LG, Haxby JV (1994) 'What' and 'where' in the human brain. Current opinion in neurobiology 4:157-165.
Wade AR, Rowland J (2010) Early suppressive mechanisms and the negative blood oxygenation level-dependent response in human visual cortex. J Neurosci 30:5008-5019.
Van Essen DC, Newsome WT, Maunsell JH, Bixby JL (1986) The projections from striate cortex (V1) to areas V2 and V3 in the macaque monkey: asymmetries, areal boundaries, and patchy connections. The Journal of comparative neurology 244:451-480.
van Hateren JH, van der Schaaf A (1998) Independent component filters of natural images compared with simple cells in primary visual cortex. Proceedings Biological sciences / The Royal Society 265:359-366.
Vanni S (2012) Local model for contextual modulation in the cerebral cortex. Neural Networks 25:30-40.
Vanni S, Rosenstrom T (2011) Local non-linear interactions in the visual cortex may reflect global decorrelation. J Comput Neurosci 30:109-124.
Vanni S, Rosenström T (2011) Local non-linear interactions in the visual cortex may reflect global decorrelation. Journal of Computational Neuroscience.
Wassle H, Boycott BB (1991) Functional architecture of the mammalian retina. Physiological reviews 71:447-480.
Webb BS, Dhruv NT, Solomon SG, Tailby C, Lennie P (2005) Early and late mechanisms of surround suppression in striate cortex of macaque. J Neurosci 25:11666-11675.
Williams AL, Singh KD, Smith AT (2003) Surround modulation measured with functional MRI in the human visual cortex. Journal of Neurophysiology 89:525-533.
Williams SR, Stuart GJ (2002) Dependence of EPSP efficacy on synapse location in neocortical pyramidal neurons. Science 295:1907-1910.

Vinje WE, Gallant JL (2000) Sparse coding and decorrelation in primary visual cortex during natural vision. Science 287:1273-1276.
Vinje WE, Gallant JL (2002) Natural stimulation of the nonclassical receptive field increases information transmission efficiency in V1. Journal of Neuroscience 22:2904-2915.
Xing J, Heeger DJ (2001) Measurement and modeling of center-surround suppression and enhancement. Vision Research 41:571-583.
Yau KW (1994) Phototransduction mechanism in retinal rods and cones. The Friedenwald Lecture. Invest Ophthalmol Vis Sci 35:9-32.
Zenger-Landolt B, Heeger DJ (2003) Response suppression in V1 agrees with psychophysics of surround masking. Journal of Neuroscience 23:6884-6893.
Zonta M, Angulo MC, Gobbo S, Rosengarten B, Hossmann KA, Pozzan T, Carmignoto G (2003) Neuron-to-astrocyte signaling is central to the dynamic control of brain microcirculation. Nat Neurosci 6:43-50.
Zuiderbaan W, Harvey BM, Dumoulin SO (2012) Modeling center-surround configurations in population receptive fields using fMRI. J Vis 12:10.

Aalto-DD 193/2015

ISBN 978-952-60-6529-8 (printed)
ISBN 978-952-60-6530-4 (pdf)
ISSN-L 1799-4934
ISSN 1799-4934 (printed)
ISSN 1799-4942 (pdf)

Aalto University
School of Science
Department of Neuroscience and Biomedical Engineering
www.aalto.fi

BUSINESS + ECONOMY

ART + DESIGN + ARCHITECTURE

SCIENCE + TECHNOLOGY

CROSSOVER

DOCTORAL DISSERTATIONS